UNIVERSITÀ DEGLI STUDI DI MILANO
Facoltà di Medicina e Chirurgia
Dipartimento di Farmacologia, Chemioterapia e Tossicologia Medica

Dottorato di ricerca in Biotecnologie Applicate alle Scienze Mediche
XXIV ciclo

hnRNP K: A NEW PROTEIN IN NEURON DEVELOPMENT AND FUNCTION

Tesi di Dottorato di Ricerca di:
Alessandra Folci

Coordinatore: Prof. Enrico Ginelli
Correlatore: Prof. Diego Fornasari
Tutor Dott.ssa Maria Passafaro

Anno Accademico 2010-2011

INDEX

1 INTRODUCTION

1.1 RNA BINDING PROTEINS

RNA binding proteins (RBPs) are proteins able to form dynamic interactions with coding, untranslated and non–protein-coding RNAs in functional units called ribo- nucleoprotein (RNP) complex. RBPs interact directly with RNA molecules through specific domains called RNA binding domains and are a key component in RNA metabolism, regulating all aspects of RNA biogenesis from RNA maturation, surveillance, nucleocytoplasmic transport to subcellular localization, translation and RNA degradation (Glisovic et al., 2008).

Humans have >500 RBPs (Anantharaman et al., 2002), each interacting, with different affinities, with RNA. RBPs are characterized by the presence of RNA binding domains (RBDs) containing 60–100 residues. These domains are found in single or multiple copies and usually associate with RNA in a sequence- and structure-dependent manner. More than 40 RBDs have been identified to date – the most common class being the RNA recognition motif (RRM), found in >50% of the RBPs. A well-characterized RRM-domain containing RBP is the poly(A)-binding protein (PABP), which binds to the 30 poly(A) sequence of mRNAs. Other common RBDs include the K homology (KH) domain and the Piwi/Argonaute/Zwille (PAZ) domain (Lunde et al., 2007).

Recent proteomic studies have identified additional processes in which RBPs are involved. For instance, RBPs were enriched as substrates of the ATM (ataxia telangiectasia mutated) and ATR (ATM and Rad3-related) kinases on induction of the DNA damage response (Matsuoka et al., 2007). These studies suggest that the lack of RBPs influences cell cycle checkpoint defects, genomic instability and cancer. Interestingly, RBPs were found to interact with focal adhesions proteins in a cellular attachment–dependent manner in new structures, termed the spreading initiation centers (SICs) identifying a potential new role for RBPs in cell attachment and hence cancer metastasis (de Hoog et al., 2004). Indeed, inactivation of RBP heterogeneous nuclear ribonucleoprotein (hnRNP) K prevented cell migration. Furthermore, reduced expression of Sam68 decreases cell migration and tumor metastasis in mice (Lukong et al., 2008). Additional roles of RBPs have been observed in posttranscriptional regulation. RBP Lin28, a posttranscriptional

regulator of mRNA translation and stability, was recently shown to regulate the biogenesis of let-7 microRNA (miRNA) in stem cell differentiation and in cancer (Lukong K. E.,2008).

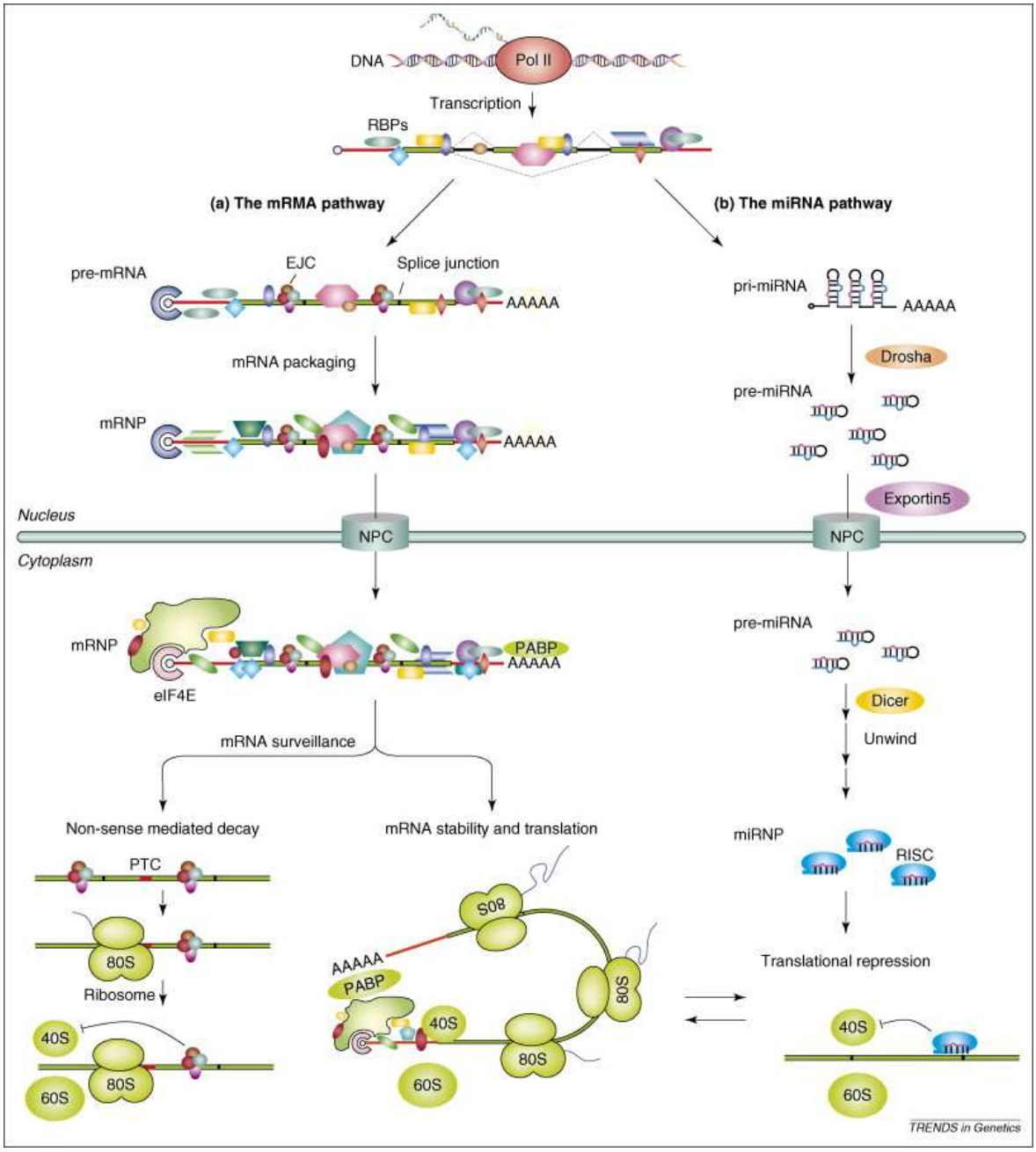

Fig.1 The functions of RNA binding proteins in eukaryotes. (a) The mRNA pathway. (b) The miRNA pathway.

1.1.2 Human diseases associated with aberrant RBP function

Considering that RBPs coordinate the elaborate networks of RNA–protein and protein–

protein interactions that control RNA metabolism, is clear that any alteration in this proteins function can impact many different genes and pathways, leading to complex and multifaceted phenotypes. Interestingly, neurodegenerative disorders are the principal clinical manifestation of RBP defects, because of the high prevalence of alternative splicing in the brain, a major function fulfilled by RBPs (Gabut et al., 2008).

Diseases associated with aberrant RBP function could be grouped into RBP loss-of-function or toxic RNA gain-of- function. A loss-of-function is observed when genetic changes or autoimmune anti- bodies lead to the inactivation of RBPs. For example, a trinucleotide repeat (CGG) expansion in the 50 -untranslated region (UTR) of the fragile X mental retardation (FMR1) gene results in the loss-of-function of the FMRP causing fragile X syndrome (FXS) (Chelly and Mandel, 2001). The toxic RNA gain- of-function is usually observed when microsatellite-expansion repeats are transcribed into mRNAs resulting in the entrapment of RBPs that associate with the repeats and interfere with the normal function of RBPs. A well-known example is in myotonic dystrophy type 1 (DM1), in which a CUG trinucleotide expansion in the 30 -UTR of the myotonic dystrophy protein kinase (DMPK) mRNA, results in the entrapment and loss- and gain-of-function of the RBPs muscleblind-like protein 1 (MBNL1) and CUG-binding protein 1 (CUGBP1), respectively (Wang and Cooper, 2007). In addictions to these two examples there are many neurological disorders linked with alterations in RNA binding proteins like Alzheimer disease caused by excessive protein aggregation (Higashi et al., 2007); spinal muscular atrophy (SMA), amyotrophic lateral sclerosis (ALS) (Neumann et al., 2006).

Disease	Molecular defects	RNA metabolism defects
RBP loss-of-function		
DKC	Mutations in *TERC* and *TERT*	Defects in RNP telomerase activity
FXS[a]	CGG repeats >200 in 5′ UTR of *FMR1* gene	Protein translation
Hu syndrome[a]	Autoantibodies targeting Hu RBPs	mRNA stability and mRNA export
MRS and NSMR	Mutations in *UPF3B*	Defect in NMD surveillance
POMA[a]	Autoantibodies targeting Nova RBPs	Alternative splicing
PWS	Deletion of *SNURF* locus	Splicing
RP	Deletion or mutations in *PRPF31, PRPF8, HPRP3*	SnRNP assembly
SMA[a]	Deletion/ mutations of the *SMN1*	RNP assembly and RNP localization
RNA gain-of-function		
DM1[a]	CUG-repeat expansion in 3′ UTR of *DMPK*	Alternative splicing; toxic mRNA; RBP entrapment
DM2[a]	CCTG-repeat expansion in intron 1 of *ZNF9*	Alternative splicing; toxic mRNA; RBP entrapment
FXTAS[a]	CGG-repeats 55–200 in 5′ UTR of *FMR1*	Toxic mRNA; RBP entrapment
HDL-2	CUG-repeat expansion within the junctophilin-3 gene	RBP entrapment
OPMD[a]	GCG trinucleotide expansion in *PABP2*	Polyadenylation
SCA[a]	CAG- or CTG-repeat expansions in *SCA*	Splicing

Fig.2 Disease implications of RBPs and RNA metabolism

1.2 hnRNP K PROTEIN

HNRNPK gene encodes for heterogeneous nuclear ribonucleoprotein K (hnRNP K) and is mapped in humans chromosome 9 (Dejgaard et al., 1994); hnRNP K belongs to the heterogenous nuclear ribonucleoproteins (hnRNPs) family which includes RNA-binding proteins (RBP) containing multiple K homolgy (KH) domains that are most completely conserved between Xenoopus leavis and mammalas (Siomi et al., 1993). Four alternatively spliced human K transcripts are known that result from alternative use of regulatory sites in the 30 exons (Dejgaard et al., 1994). Another splicing variant is now thought to be the previously designated hnRNP J and represents K protein transcript without one exon between the regions coding KH1 and KH2 domains. Differential function, if any, of K protein isoforms remains to be defined.

1.2.1Structure of hnRNP K

Human hnRNP K includes three KH domains denoted KH1, KH2, and KH3 that allow the bind with RNA and DNA (Braddock et al., 2002). The K-homology (or KH domain) was first identified in the protein hnRNP K, which gave the domain its name, but is also presented in several RNA-binding proteins, tipically in multiple copies as in in FMRP, but also in single copy like in Sam68. The KH domain can recognize both ssRNA and ssDNA, and is involved in a wide range of processes that include translation, splicing, transcription, and even chromatin remodeling (Bomsztyk et al., 2004). The KH domain is not restricted to eukaryotes—it is also found in eubacteria and archaea. The KH domain is about 70 amino acids long and consists of a three- stranded β-sheet packed against three α-helices and is subdivided into two subfamilies: type I (βααββα) is mostly found in eukaryotic proteins and type II (αββααβ) in prokaryotic proteins(Bomsztyk et al., 1997).

The KI domain (K-protein interactive region) is sandwiched between KH2 and KH3. A series of proline-rich docking sites in the KI domain (P-p-X-P) are responsible for the ability of hnRNP K to interact with the SH3 domains of the oncogenic Src family of tyrosine protein kinases; SH3 domains are found in several proteins involved in signal transduction pathways that regulate cytoskeletal architecture or cellular proliferation (Bomsztyk et al., 1997). In addicion hnRNP K contains a nuclear localization signal (NLS)and a nuclear

shuttling domains (KNS). This domain allows shuttling between nuleos and cytosplasm. Thanks to ist ability to interacts with many different molecules, both proteins and nucleic acids, this protein result to be involved in a variety of intracellular signal transduction pathways (Bomsztyk et al., 2004).

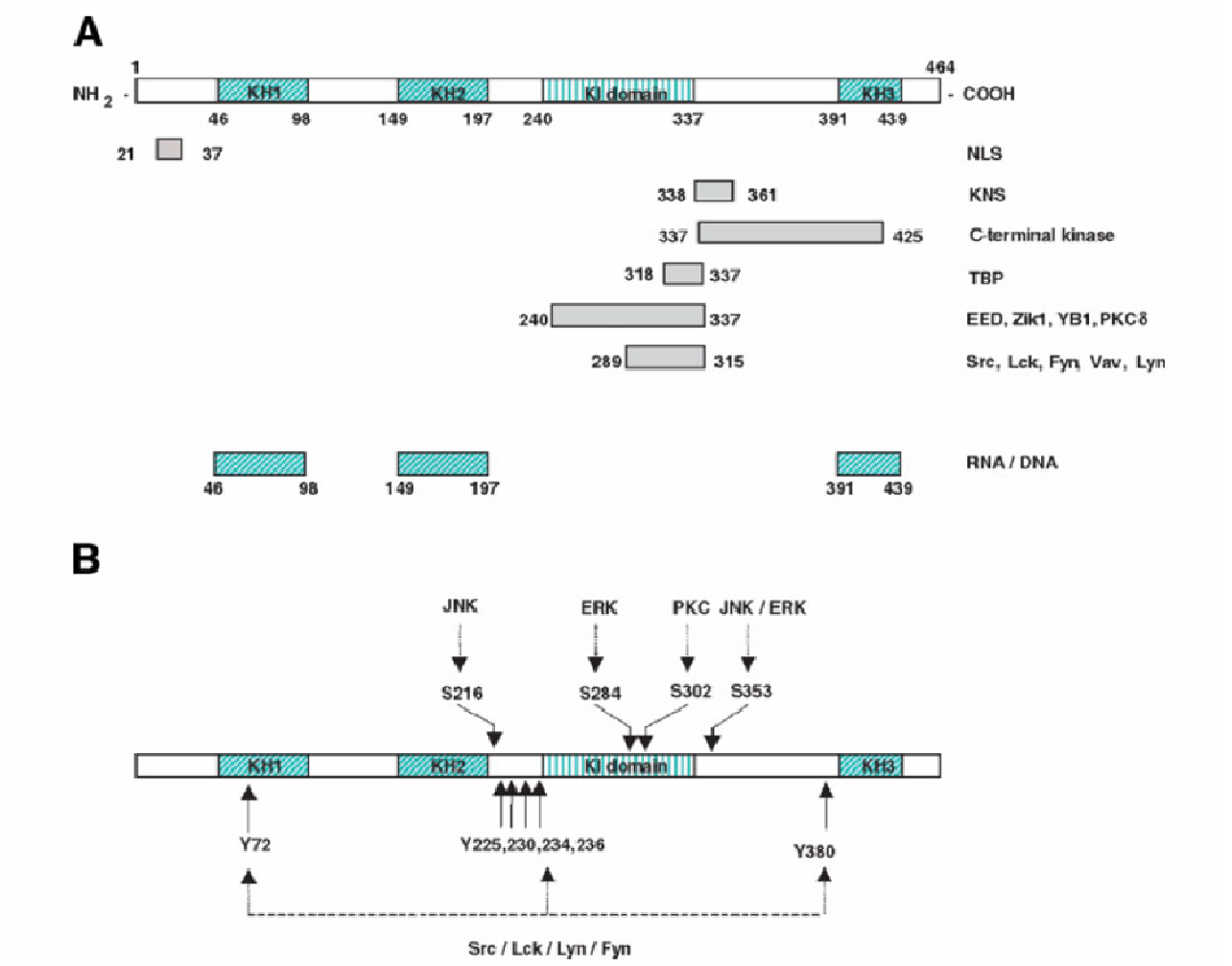

Fig. 3 hnRNP K modular structure (A) and sites targeted by kinase cascades (B). **A)** The rectangles represent K homology domains (KH), K interactive region (KI), nuclear localization signal (NLS), nuclear shuttling domain (KNS), and domains that recruit protein and RNA partners. Numbers indicate positions of amino acid residues. **B)** Arrows show serine, S, and tyrosine, Y, amino acids that are targeted by c-Src, PKC, ERK1/2 and JNK cascades. Numbers in A and B indicate positions of amino acid residues (Bomsztyk et al., 2004).

1.2.2 K protein involvement in multiple steps that compose gene expression

hnRNP K protein interacts with diverse groups of molecular partners and is found in multiple subcellular compartments. For the majority of these protein–protein interactions, the functional relevance remains to be tested. Nonetheless, the diversity of hnRNP K interactions predicts that K protein is involved in multiple processes that compose gene expression, such as chromatin remodeling, transcription, splicing, translation and mRNA stability. Involvement of hnRNP K in gene expression has been shown in many studies. Chromatin immunoprecipitations reveal that K protein interaction with gene loci is genome-wide. hnRNP K is found in higher density at transcribed compared to silent gene loci (Ostrowski et al., 2003).

Moreover many studies provide evidence that hnRNP K binds the CT element present within the c-myc P1 promoter in vitro. Overexpression of K protein increases activity of the c-myc gene promoter (Michelotti et al., 1996).

hnRNP K interacts with factors involved in RNA splicing; involvement of this protein in splicing was demonstrated for the chicken b-tropomyosin gene where the alternative splicing of exon 6A is augmented by downstream intronic enhancer element. hnRNP K was characterized as a component of this intronic enhancer complex that activates splicing of this alternative exon (Expert-Bezancon et al., 2002).

K protein is also involved in regulation of message stability and translation.

For example, K protein along with five other proteins, including YB-1 and hnRNP E1, binds to the 3' UTR of the rennin mRNA and regulates its stability. The interaction of K protein with YB-1(26) and hnRNP E1 may provide an avenue for signaling this process by extracellular events since YB-1 and hnRNP E1 are substrates of very few kinases while K protein is a target of many (Bomsztyk et al., 2004).

The mechanisms of K protein action are best studied in translation. One of the first clues that K protein might be involved in translation came from the observation that K protein binds the translation elongation factor-1a (EF-1a). Subsequently several studies provided direct evidence for the role of K protein in translational regulation (Bomsztyk et al., 2004).

1.2.3 hnRNP K in neurons

Given this wide variety of nucleic acid and protein interactions one might assume that hnRNP K is ubiquitously expressed, while an earlier report indicated that hnRNP K protein is expressed in several tissues, including brain, but the level of expression change in different cell type (Kamma et al., 1995). Moreover the hnRNP K expression is different in the development stages. In the central nervous system, hnRNP K mRNA expression gradually decreases during development until it is restricted to a very limited number of structures including most notably hippocampus and retina. In contrast to the central nervous system, hnRNP K in the peripheral nervous system remains high throughout embryonic development with dramatic expression in several peripheral ganglia. At embryonic day 14 (E14), hnRNP K mRNA and protein is highly expressed throughout the developing nervous system being seen in the telencephalon, hippocampal formation, septum, basal ganglia, pre-optic area, diencephalon, mesencephalon, rhombencephalon and spinal cord. hnRNP K is also highly expressed in E14 dorsal root ganglia and retina; from E18, hnRNP K mRNA levels in general are lower although still readily detectable. At postnatal day 30 (P30) there is a dramatic decrease in hnRNP K expression in the brain. In fact, hnRNP K mRNA was detected only in the retrosplenial granular cortex, the secondary visual cortex, the dentate gyrus and the CA1, CA2, and CA3 regions of the hippocampus (Blanchette et al., 2006). This finding is coupled with a work in which hnRNP K was demonstrated to interact directly with HuB, an RNA-binding protein required for neuronal differentiation (Yano et al., 2005). The hnRNP K/HuB interaction appears to play a critical role in the switch from proliferation to neuronal differentiation by regulating, post-transcriptionally, the mRNA encoding p21, a cyclin-dependent kinase inhibitor known to positively regulate neuronal differentiation (Yano et al., 2005). Thus, knowledge of hnRNP K expression within the nervous system is likely to have implications for a molecular understanding of neuronal differentiation and neuron-specific gene expression.

In the past year a new work of Proepper C (Proepper et al.) showed the interaction of hnRNP K with Abelson-interacting protein 1 (Abi-1) in postsynaptic sites. In this paper Proepper hypothesized possible involvement in spine morphology.

In the last few years other papers suggested a possible role of hnRNP K in neuron development e function. Liu Y. in two different papers described how hnRNP K is essential for axon outgrowth in Xenopus: suppressing hnRNP K expression the axonal

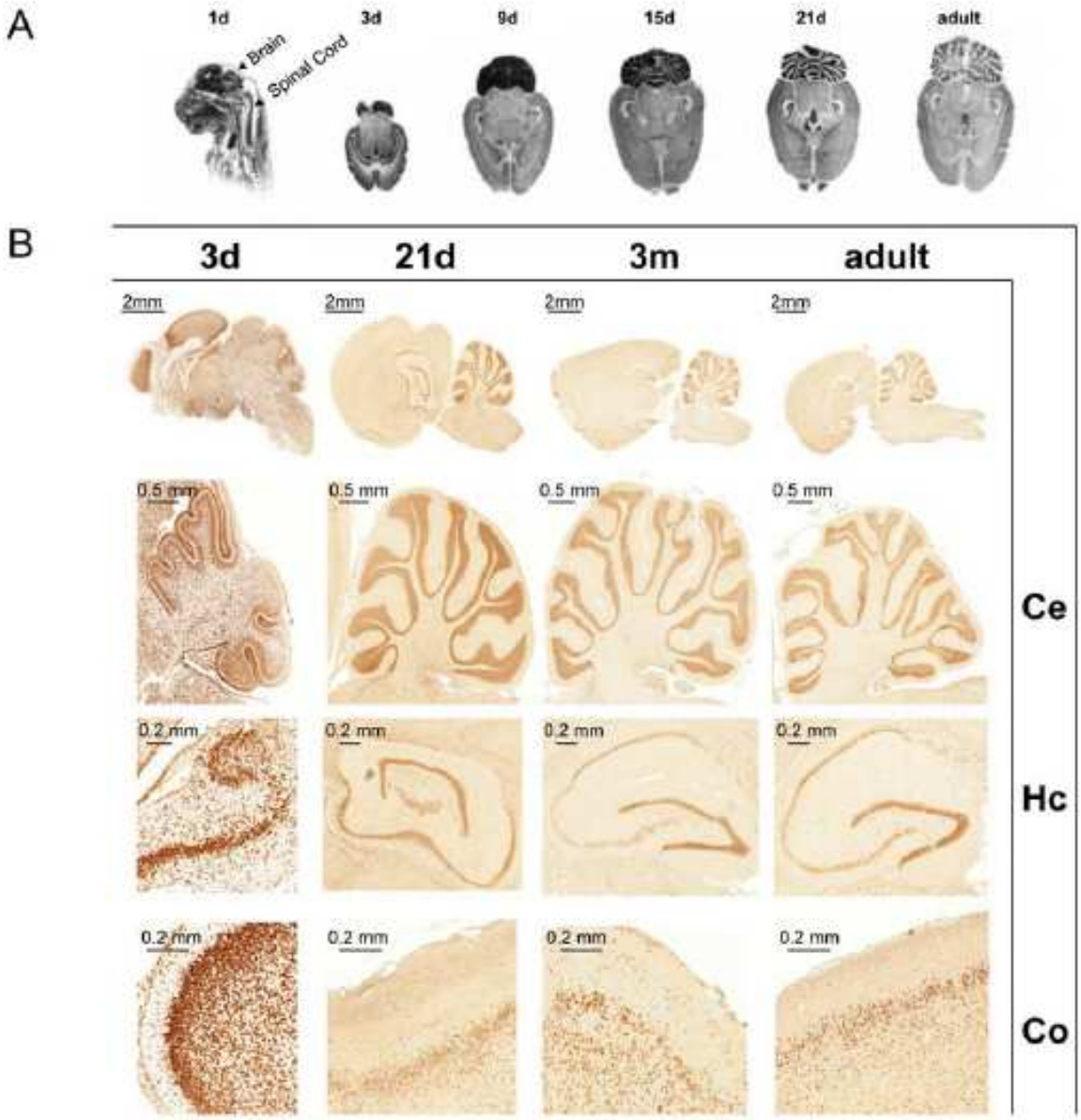

Fig. 4 (A) In situ hybridization of hnRNPK mRNA during rat brain development. At embryonic time points (1d), the mRNA of hnRNPK can easily be detected in all areas of the developing brain including the spinal cord. At later stages of maturation (horizontal sections, 3d-adult), the expression levels decrease and become more and more restricted to the cortex (Co), the hippocampal formation (Hc) and the granular layer of the cerebellum (Ce). (B) Immunohistochemical detection of hnRNPK in rat brain sagittal sections. At early time points of brain development (3d), a predominant nuclear labeling of hnRNPK can be detected in nearly all neurons. Again, cortex, hippocampus and cerebellum are most strongly labeled. At later time points, differences in spatial expression become even more prominent and intense staining is especially seen in granule cells of the cerebellum (Ce) and the dentate gyrus as well as in the CA1-4 regions of the hippocampus. In the cortex (Co), the staining intensity diminishes at later stages and only some scattered neurons in deeper cortical layers remain positive for hnRNPK (Proepper et al.)).

outgrowth is blocked and is also inhibited the translation of NF-M (medium neurofilament). These observations are consistent with the hypothesis that hnRNP K plays an essential role in the translation of a subset of proteins involved in building the axon (Liu et al., 2008). In a following paper he showed a pattern of cytoskeletal gene post-trascriptionally regulated by hnRNP K, including actin related protein 2 (Arp2) (Liu and Szaro). Arp 2 is a component of Arp2/3 complex, a powerful nucleator of actin filaments (Goley and Welch, 2006).

The involvement of hnRNP K in actin dynamic is also supported by the interaction in heterologous cells with Wiskott-Aldrich syndrome protein (N-WASP) (Yoo et al., 2006) another key player in actin polymerization pathway through its positive interaction with Arp2/3 complex (Goley and Welch, 2006).

Taken together all these findings show an increasing interest in hnRNP K involvement in neuron development and function with particular attention on its role in actin dynamics.

1.3 Arp2/3 COMPLEX AND ACTIN CYTOSKELETON

The eukaryotic actin cytoskeleton has an important role in remarkably diverse processes, including cell migration, endocytosis, vesicle trafficking and cytokinesis, many of which are essential for the survival of the cell. The core constituent of the actin cytoskeleton is monomeric globular (G)-actin, a 43-kDa ATPase that can self-assemble into filamentous (F)-actin. Each asymmetric filament possesses a fast growing barbed end and a slower growing pointed end that are distinguishable by their structural characteristics and kinetic properties. ATP hydrolysis in the filament is tightly coupled to polymerization and regulates the kinetics of assembly and disassembly, as well as the association of interacting proteins (Pollard and Borisy, 2003). The dynamic assembly and disassembly of filaments and the formation of larger scale filament structures are crucial aspects of actin's function, and are therefore under scrupulous control by over a hundred actin-binding proteins, including the protein of Arp2/3 complex. Arp2/3 complex has been shown to have a crucial role in the formation of branched-actin-filament networks during diverse processes ranging from cell motility to endocytosis (Goley and Welch, 2006).

Arp2/3 complex is a seven-subunit protein that plays a major role in the regulation of the actin cytoskeleton. Two of its subunits, the Actin-Related Proteins ARP2 and ARP3 closely

resemble the structure of monomeric actin and serve as nucleation sites for new actin filaments.

Members of the Wiskott-Aldrich syndrome protein (WASP) family, including WASP, neural WASP (N-WASP), and WASP-family verprolin homologous proteins (WAVEs), are emerging as critical regulators of the actin cytoskeleton. These proteins initiate the nucleation of new actin filaments through activation of the Arp2/3 complex (Rohatgi et al., 1999). New filaments generated by the Arp2/3 complex are formed at fixed angles to the mother filament, creating a branched actin network that is commonly found in protrusive regions of cells . C-terminal sequences within N-WASP, consisting of a verprolin-like homology domain (V), a central domain (C), and an acidic region (A), mediate binding of G-actin and the Arp2/3 complex to these proteins, which subsequently results in actin nucleation (Goley and Welch, 2006).

N-WASP, as its name implies, is highly expressed in the brain, but its function in the nervous system is not well understood (Miki et al., 1996).

1.3.1 Actin cytoskeleton in dendritic spines

The actin cytoskeleton plays a major role in morphological development of neurons and in structural changes of adult neurons, in fact many structures in neurons have an actin cytoskeleton, including dendritic spines (Hotulainen and Hoogenraad).

Dendritic spines are small actin-rich protrusions from neuronal dendrites that form the postsynaptic part of most excitatory synapses and are major sites of information processing and storage in the brain. Early electron microscopy studies have shown that actin is the major cytoskeletal component of dendritic spines (Landis and Reese, 1983).

In mature spine, the base, neck, and head all consist of a mixture of branched and linear actin filaments; the neck contains different ratios of both linear and branched filaments, whereas most branched actin filaments localize to the distal regions of the spine head (Korobova and Svitkina). Actin filaments in the spine head are very dynamic and show a high turnover by continuous treadmilling (Honkura et al., 2008). In this way the actin cytoskeleton of mature dendritic spines, especially of the spine head, resembles actin structures found in lamellipodia. Arp2/3 complex is concentrated in spines (Racz and Weinberg, 2008) and its knockdown from hippocampal neurons revealed its importance in dendritic spine head formation (Hotulainen et al., 2009). Depletion of the Arp2/3 complex

activators, including cortactin, Abi2, WAVE-1 (WASP-family verprolin homology protein-1), N-WASP (neural Wiskott-Aldrich syndrome protein), and Abp1 (actin-binding protein 1) alters the morphology and number of spines (Hotulainen and Hoogenraad). Consistently, WAVE-1 and Abi2 knock-out mice show hippocampal-dependent learning and memory deficits (Hotulainen and Hoogenraad).

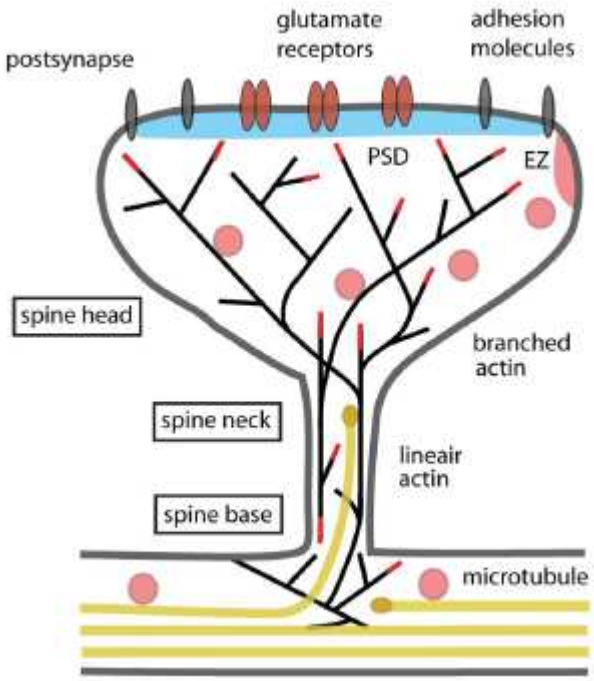

Fig. 5 Schematic diagram of a mature mushroom-shaped spine Dendritic spines exhibit a continuous network of both straight and branched actin filaments (black lines). The actin network is spread in the spine base, gets constricted in the neck, undergoes extensive branching at the neck–head junction, and stays highly branched in the spine head. The actinpolymerizing barbed ends are indicated as red lines. Stable microtubule arrays are predominantly present in the dendritic shaft. A small fraction of the microtubules in mature dendrites are dynamic and depart from the dendritic shaft, curve, and transiently enter dendritic spines. The microtubule plus-ends are symbolized as yellow ovals (Hotulainen and Hoogenraad).

1.4. Excitatory synapse

In the nervous system, a synapse is a structure that permits a neuron to pass an electrical or chemical signal to another cell; each synapse is a complex of several components: a presynaptic element, a cleft and a postsynaptic element. The presynaptic element is a

specialized part of the presynaptic neuron axon, the postsynaptic element is a specialized part of the postsynaptic somatodendritic membrane, and the space between these two closely apposed elements is the cleft.

The portion of the axon that participates is the bouton, and it is identified by the presence of synaptic vesicles and a presynaptic thickening at the active zone (Sudhof, 2004).

The active zone is the portion of presynaptic element that is apposed to the postsynaptic element and this is the region where the synaptic vesicles are concentrated, and where at any time, a small number of vesicles are docked and presumably ready for fusion. The active zone is also enriched with voltage gated calcium channels, which are necessary to permit activity-dependent fusion and neurotransmitter release. Directly apposed to the active zone (and perfectly matched with it in size and shape) is the PSD, an electron-dense thickening of the postsynaptic membrane, where glutamate receptor channels and their associated signaling proteins are highly concentrated. The presence of a prominent PSD is characteristic of glutamatergic synapses (hence they are termed asymmetric); in contrast, inhibitory (symmetric) synapses lack a prominent postsynaptic thickening (Sheng and Hoogenraad, 2007). The presynaptic active zone and the PSD, which define the extent of the true synapse morphologically, are separated by a gap of 20–25 nm. A wide variety of cell adhesion molecules hold pre- and postsynaptic membranes together in register and at the appropriate separation (Scheiffele, 2003). Puncta adherens junctions and/or cadherin clusters lie adjacent to the synapse proper or may occur within the PSD-active zone apposition (Elste and Benson, 2006). The postsynaptic membrane can be divided into the PSD itself, as well as perisynaptic and extrasynaptic regions. The latter two terms are often used interchangeably, although it should be borne in mind that the perisynaptic membrane within 100 nm of the PSD probably differs in molecular content and function from the extrasynaptic membrane at greater distances from the PSD. Extrasynaptic regions have specialized postsynaptic functions and are enriched for a distinctive set of proteins, such as metabotropic glutamate receptors (Baude A. 1993) and proteins involved in endocytosis (Racz et al., 2004). On most principal neurons in the mammalian brain (e.g., pyramidal neurons of cortex and hippocampus, Purkinje cells of cerebellum, medium spiny neurons of striatum), the postsynaptic specialization is housed on tiny actin rich protrusions called dendritic spines. In contrast, inhibitory synapses are made on the shaft of the dendrite.

The PSD (and hence the synaptic contact) is typically located on the dilated tip (“head”) of the spine. The dimensions of the spine head are highly correlated with the size of the PSD and associated active zone, as well as synaptic strength (Kasai et al., 2003).

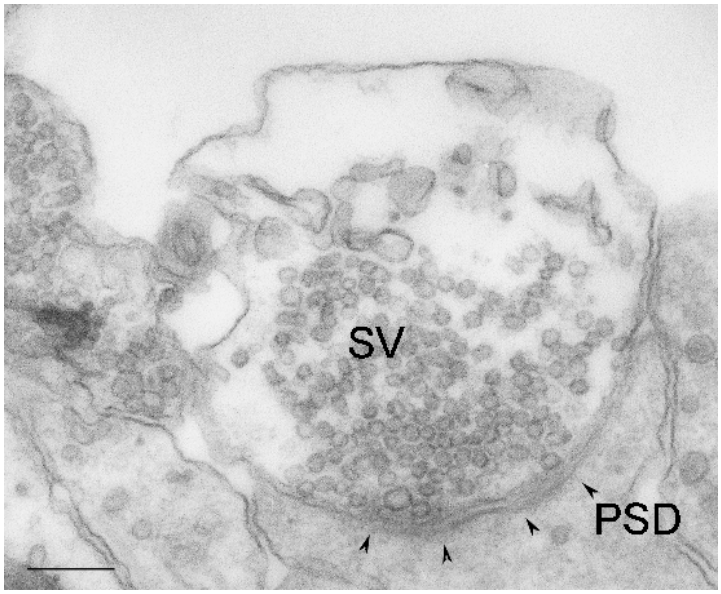

Fig. 6 EM morphology of an excitatory synapse from mouse hippocampal neurons (DIV15). The presynaptic terminal contains synaptic vesicles (SV) loaded with glutamate, facing the PSD located on the tip of the dendritic spine. The synaptic cleft separating pre- and postsynaptic membranes is 20–25 nm wide

.

1.4.1 Dendritic spine: structure, function and pathology

Dendritic spines are small (typically 0.5–2 μm in length) membranous protrusions that house the essential postsynaptic components, including the PSD, actin cytoskeleton, and a variety of “supporting” organelles. Spines occur at a density of 1–10 spines per μm of dendrite length on principal neurons, and they receive most of the excitatory synapses in the mature mammalian brain (Sheng and Hoogenraad, 2007).

The formation of new spines occurs during all life; during the early synaptogenesis, dendritic shafts are covered with filopodia, which are long narrow protrusion that are more transient and contain less F-actin than spines. Dendritic filopodia transiently extend and retract from the dendritic shaft with an average lifetime of ~10 min. Filopodia probably function to maximize the chance encounter between a developing axon and a target dendrites. Once contact is made a synapse can be initiated and proceed through

appropriate maturational steps. Such maturation requires intricate crosstalk between the nascent presynaptic and postsynaptic part of the synapse (Calabrese et al., 2006).

Each spine receives input from a single excitatory presynaptic terminal and has a head connected to the dendritic shaft by narrow neck. Depending on the shape and size, the dendritic spines are subdivided in several categories based on the relative sizes of the spine head and neck (Peters and Kaiserman-Abramof, 1970):

- Mushroom spines with a large head and narrow neck;
- Thin spines with a smaller head and narrow neck;
- Stubby spines without an obvious constriction between the head and the attachment to the shaft.

Spines are highly diverse and changes in spine size as well as in density reflect changes in the strength of synaptic transmission: spines with large heads are generally stable, express large numbers of AMPARs, and contribute to strong synaptic connections. By contrast, spines with small heads are more motile, less stable, and contribute to weak synaptic connections (Matsuzaki et al., 2004). In vivo timelapse studies show spines turn over at various rates in the mouse brain; a large fraction of mushroom spines are persistent, with lifetimes up to many months. Nevertheless, it is currently believed that a subset of spines can undergo changes in shape or number in response to experience, especially during postnatal brain development, thereby relating spine morphology to synaptic plasticity and long-term memory formation (Grutzendler et al., 2002). The size, motility, and stability of dendritic spines depend largely on actin, the primary cytoskeleton within spines. A complex network of regulatory proteins, including the Rho family GTPases, controls actin arrangement and spine morphogenesis (Sheng and Hoogenraad, 2007).

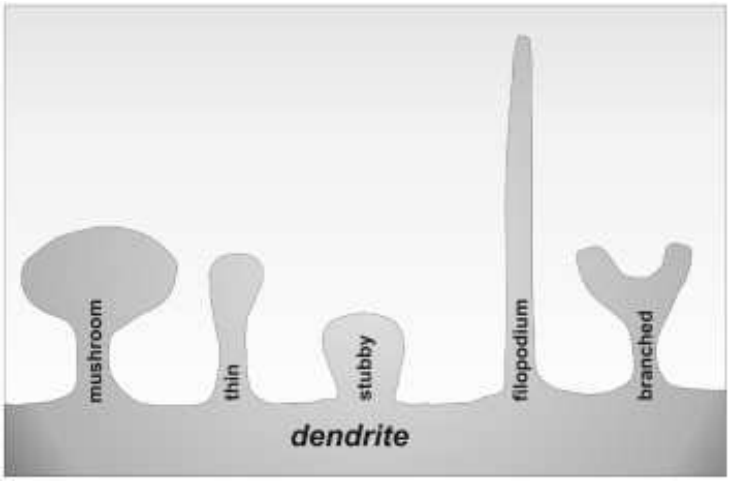

Fig. 7 Different spine categories based on the relative sizes of the spine head and neck

The number and the shape of dendritic spines are regulated by both physiological and pathological events. In fact many pathological condition leads to decreased number of dendritic spines (e.g. most form of mental retardation, poisoning, alcohol abuse, epilepsy), whereas an increase in spine densities (e.g. as seen in some types of deafferentiation or in sudden infant death syndrome) is less common (Fiala et al., 2002). About the pathological alteration of spine shape the most common condition is mental retardation, indeed is already known the link between mental retardation and alterated dendritic spine which was suggested for the first time in 1974 (Purpura, 1974). Purpura showed that mental retardation was associated with an occurrence of abnormally long, thin spines and an absence of short, thick spines on dendrites of cortical neurons in retarded children.
Moreover the spines are remarkably dynamic, in fact live imaging studies showed changing shape and size over time scale of seconds to minutes and of hours to days (Alvarez and Sabatini, 2007) and the spine turnover is a normal part of brain physiology. Spine density reaches its maximum level during late development when synaptic plasticity is at its height and that decrease to a relative stable level throughout adulthood.

1.4.2 The postsynaptic density

The postsynaptic density (PSD) is a structure composed of both membranous and cytoplasmic proteins localized at the postsynaptic plasma membrane of excitatory

synapses and can be considered a huge membrane-associated protein complex (or organelle), specialized for postsynaptic signaling and plasticity (Sheng and Kim, 2002). Proteomic studies have identified several hundred proteins that constitute the PSD, including glutamate receptors, ion channels, cell adhesion molecules, and signaling enzymes, as well as membrane trafficking, cytoskeletal and scaffolding proteins. The molecular composition of the PSD varies between different neuronal cell types and different brain regions. The PSD appears to be assembled around several key scaffold proteins, including PSD-95, which has several protein–protein interaction domains (including three PDZ domains) through which it binds to a variety of membrane, signaling, and scaffolding proteins. On the cytoplasmic side of the PSD, Shank and Homer scaffold proteins interact to form a mesh like structure. Recent electronmycroscopy studies are beginning to reveal the three-dimensional organization of the PSD and its constituent protein complexes (Sheng and Kim, 2002).

The PSD has structural and signaling roles. It localizes and stabilizes glutamate receptors and adhesion molecules in the postsynaptic membrane, thereby aiding synaptic adhesion and the alignment of neurotransmitter receptors to the presynaptic release sites. In addition, the PSD assembles a variety of signaling molecules close to glutamate receptors, so activation (particularly of NMDA receptors) is efficiently coupled to postsynaptic signaling pathways. The PSD is highly dynamic in structure and composition. Proteins move into and out of the PSD, regulated by synaptic activity. For instance, CaMKII*α* and AMPA receptors can be rapidly recruited to the PSD following synaptic stimulation. Several proteins of the PSD are turned over in response to activity via proteasomal degradation. These changes are believed to contribute to plasticity of synaptic strength and structure, such as long-term potentiation and synaptic homeostasis (Kim and Ko, 2006, Kim and Sheng, 2009).

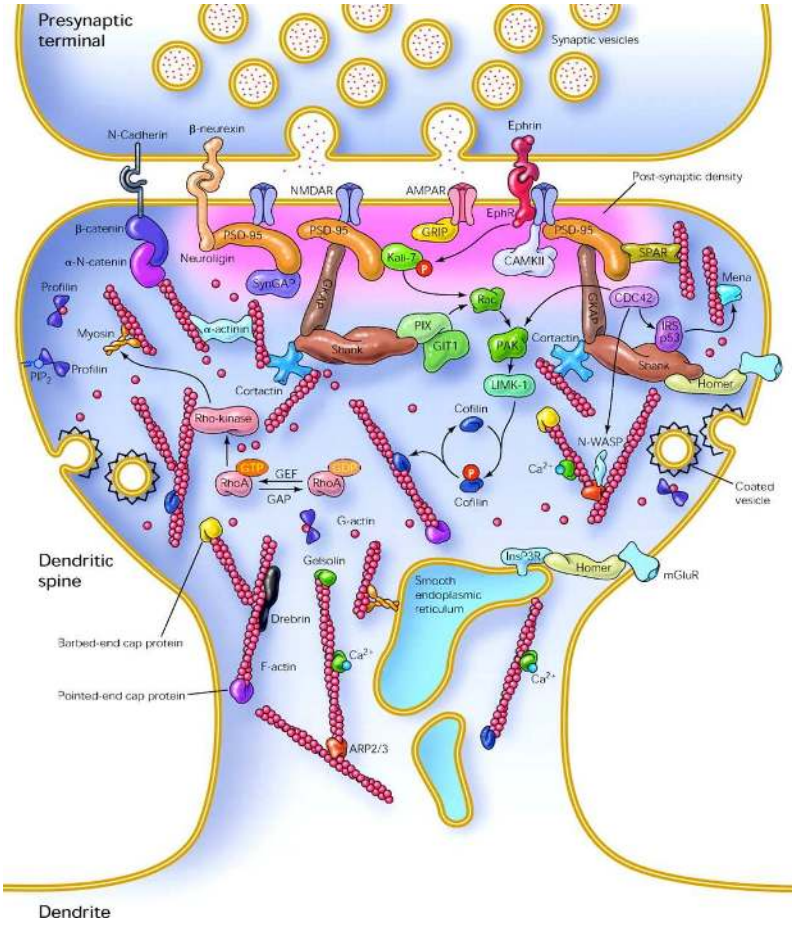

Fig. 8 Some important component of excitatory synapse (Calabrese et al., 2006)

1.5 SYNAPTIC PLASTICITY

One of the most important and fascinating properties of the mammalian brain is its plasticity; the capacity of the neural activity generated by an experience to modify neural circuit function and thereby modify subsequent thoughts, feelings, and behavior. Synaptic plasticity specifically refers to the activity-dependent modification of the strength or efficacy of synaptic transmission at preexisting synapses, and for over a century has been proposed to play a central role in the capacity of the brain to incorporate transient experiences into persistent memory traces. Synaptic plasticity is also thought to play key roles in the early development of neural circuitry and evidence is accumulating that impairments in synaptic plasticity mechanisms contribute to several prominent neuropsychiatric disorders (Citri and Malenka, 2008).

1.5.1 Long-term synaptic plasticity

It is widely believed that experience of any sort modifies subsequent behavior at least in part through activity dependent, long-lasting modifications of synaptic strength. The brain encodes external and internal events as complex, spatio-temporal patterns of activity in large ensembles of neurons that can be conceptualized as 'neural circuits'. A key feature defining the behavior of any given neural circuit is the pattern of synaptic weights that connect the individual neurons that comprise the circuit. A corollary to this hypothesis is that new information is stored (ie, memories are generated) when activity in a circuit causes a long-lasting change in the pattern of synaptic weights. This idea was put forward over 100 years ago by the Spanish Nobel laureate Santiago Ramon y Cajal, and was further advanced in the late 1940s by Donald Hebb, who proposed that associative memories are formed in the brain by a process of synaptic modification that strengthens connections when presynaptic activity correlates with postsynaptic firing (*The Organization of Behaviour* Hebb, 1949). Hebb developed his theory: when two neurons are repeatedly active at the same time, some growth occurs between them such that, at a later point in time, activity in one leads to activity in the other.

Experimental support for the very existence of such long-lasting, activity-dependent changes in synaptic strength was lacking until the early 1970s when Bliss and colleagues (Bliss and Gardner-Medwin, 1973) reported that repetitive activation of excitatory synapses in the hippocampus caused a potentiation of synaptic strength that could last for hours or even days (Citri and Malenka, 2008).

Long-term depression and long-term potentiation are two forms of long-term plasticity; in particular long-term potentiation (LTP) is a long-lasting enhancement in signal transmission between two neurons that results from stimulating them synchronously. LTP is widely considered one of the major cellular mechanisms that underlies learning and memory. By contrast LTD is a long lasting decrease in the response of neurons to stimulation of their afferents following a brief patterned stimulus.

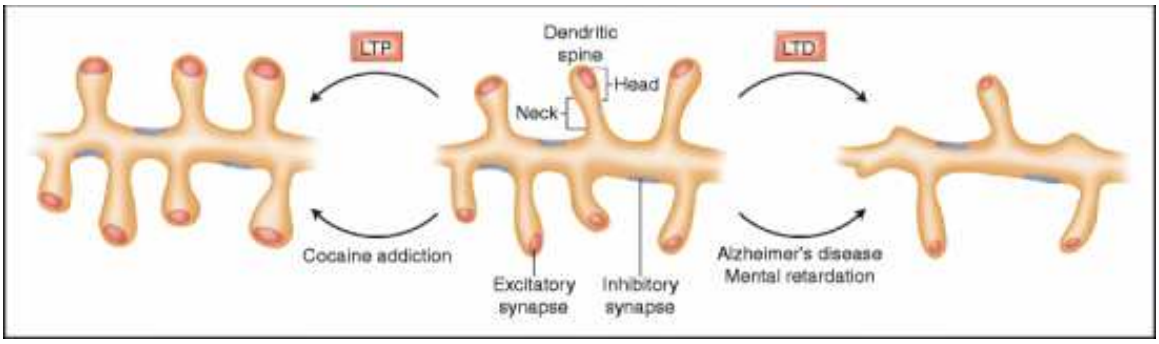

Fig. 9 The lower panel shows major morphologic events occurring in dendritic spines upon long-term potentiation (LTP; left) or long-term depression (LTD; right). In Alzheimer's disease and mental retardation, signaling cascades are triggered similar to LTD, leading to thinner, immature spines. In contrast, cocaine addiction shows similarities to LTP, resulting in bigger, mushroom-shaped, mature spines. The molecular and morphologic changes in the synapse are hallmarks of the disease pathology and are responsible for the cognitive alterations in neuropsychiatric diseases.

1.5.2 Long-term potentiation

In 1973 it was discovered that brief tetanic stimulation produced a long lasting form of synaptic plasticity, long-term potentiation (LTP), that can last for hours or days in the mammalian hippocampus. Just before that the involvement of the hippocampal formation in memory was established by clinical data indicating that lesions of this structure in humans produce anterograde amnesia. Since then, many laboratories have been studying LTP as a cellular model for information storage in the brain. Although the relation of LTP to learning is not universally accepted, LTP is a widely used and helpful paradigm for long-term synaptic plasticity in a central synapse. Based on duration and biochemical mechanisms, LTP has been subdivided into three distinct phases that have been termed LTP1, 2, and 3, or early (E)-, intermediate (I)-, and late (L)-LTP . LTP1 is a short-lasting (1 h) early form of LTP that requires post-translational modification of synaptic proteins but is protein synthesis-independent. LTP2 is slowly decaying (1–3 h) and dependent on protein translation but does not require gene transcription. Finally, LTP3 represents the long-lasting phase of LTP (hours,weeks) and is both translation- and transcription-dependent. Since LTP causes functional as well as structural changes, it can be regarded as a plastic process par excellence. In the central nervous system, excitatory inputs typically terminate on dendritic spines. It is well known that afferent synaptic activity regulates the morphology

of spines and that morphological plasticity of spines, in turn, contributes to the changes in synaptic transmission (Jedlicka et al., 2008).

LTP furthermore nicely relates to neural network theories of brain function because it implements a local learning rule, an essential element for associative neuronal networks, and one that ensures many of the computational features that make neural networks so attractive. Although there have been reviews of the role of morphological changes of spines in LTP, a recent flurry of work, much of it using novel imaging techniques and time-lapse recordings, has added important information. In addition, there is now increasing biophysical evidence of the relation between morphological and functional parameters of the spine. We now know that the volume of the spine-head is directly proportional to the number of postsynaptic receptors (Nusser et al., 1998) and to the presynaptic number of docked vesicles (Schikorski and Stevens, 1999). Also, the small size of the spine head determines fast diffusional equilibration for calcium, whereas the length of the spine neck controls the time constant of calcium extrusion in spines (Majewska et al., 2000, Yuste et al., 2000). This implies that the morphology of a spine directly reflects its function, and this makes it particularly relevant to investigate morphological changes of spines during synaptic plasticity.

1.5.3 Morphological plasticity of dendritic spines

Besides LTP, there are many different experimental or behavioral conditions that have been associated with changes in spine morphology. Many, but not all, of these studies indicate that increases of neural activity produce more spines. For example, light deprivation in mice causes a reversible reduction in the number of spines (Globus and Scheibel, 1967, Valverde, 1967, Valverde, 1971). Similarly, increases in spine density occur after visual stimulation (Parnavelas et al., 1973). Other environmental manipulations, such as rearing animals in complex environments, also alter spine morphology (Greenough and Volkmar, 1973), so do social isolation (Connor et al., 1982) and reportedly even space flight. A reduction in the size of the spine has also been observed after the first orientation flight in honeybees (Brandon and Coss, 1982). In birds, spine morphological plasticity is observed during postnatal development, imprinting with light and in learning tasks involving pecking (Yuste and Bonhoeffer, 2001). Finally, in a fascinating study, squirrels have been documented to lose 40% of their spines during hibernation and

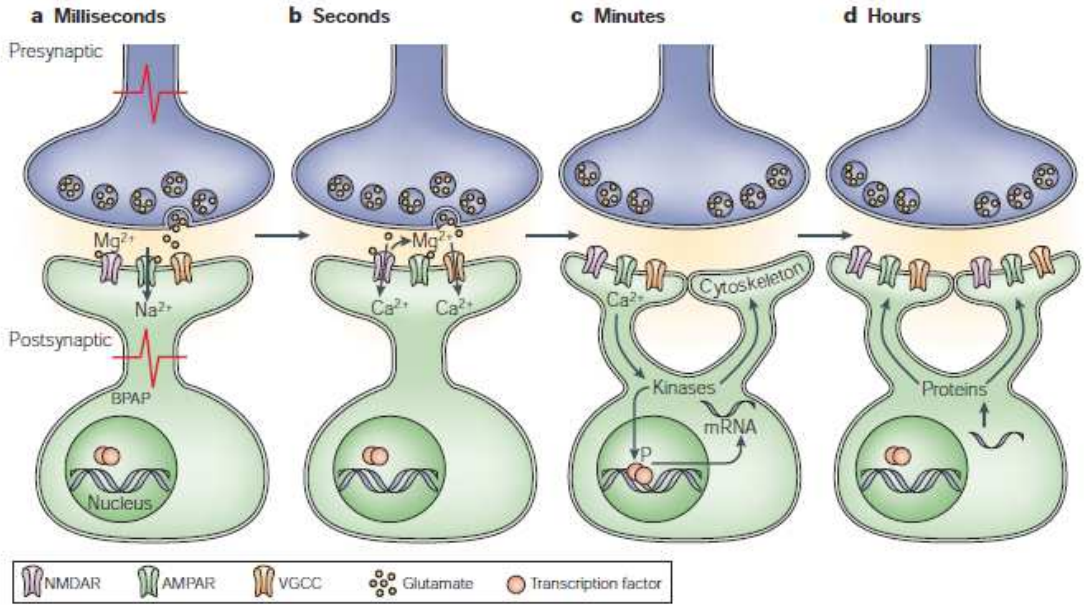

Fig. 10 Molecular mechanisms involved in the initiation and maintenance of synaptic plasticity**. a)** Activity-dependentrelease of glutamate from presynaptic neurons leads to the activation of AMPA receptors and to the depolarization of the postsynaptic neuron. Depolarization occurs locally at the synapse and/or by back-propagating action potentials. **b)** Depolarization of the postsynaptic neuron leads to removal of NMDA receptor inhibition, by Mg2+, and to Ca2+ influx through the receptor. Depolarization also activates voltage-gated calcium channels, another source of synaptic calcium. **c)** Calcium influx into the synapse activates kinases which, in turn, modulate the activity of their substrates. These substrates contribute to local changes at the synapse, such as morphological alteration through cytoskeletal regulation or induce the transcription of RNA in the nucleus by regulating transcription factors. **d)**Transcribed mRNA is translated into proteins that are captured by activated synapses and contribute to stabilization of synaptic changes. VGCC, voltage-gated calcium channel (Lamprecht and LeDoux, 2004).

to recover them in a few hours after arousal from hibernation (Yuste and Bonhoeffer, 2001).

Changes in spine form and number have also been observed in vitro. In dissociated cultures (Papa et al., 1995) as well as in brain slices (Kirov et al., 1999), pyramidal neurons have increased spine densities compared to those found in vivo. Pharmacological manipulations also influence spine morphology and number. Stimulation of AMPA receptors is needed for the maintenance of spines, whereas blocking AMPA receptors reduces the number of spines (McKinney et al., 1999). Alternatively, synaptic blockade with high Mg2+ and low Ca2+ increases both spine number and size (Kirov et al., 1999). This is also found in cultured neurons disinhibited with bicuculline (Papa et al., 1995)and

after stimulation of internal calcium release. Early on it was noticed that spines are initially overproduced and later reduced in number during normal development and aging. More recently it turned out that even during the estrous cycle of some mammals, large numbers of spines are produced in the hippocampus and later eliminated in substantial numbers. Finally, many diseases, such as dementia, mental retardation, Down syndrome, irradiation, malnutrition, fragile X syndrome, and epilepsy, can produce abnormalities in spine morphologies(Yuste and Bonhoeffer, 2001).

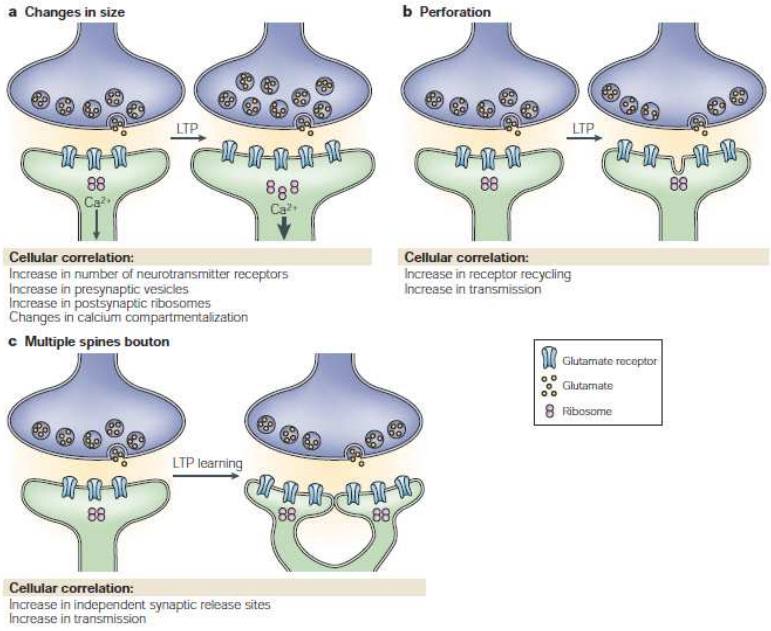

Fig. 11 Long-term potentiation (LTP) or learning induces morphological changes in dendritic spines. **a)** Increase in spine head volume and widening and shortening of spine neck. **b)** Spine perforation. **c)** Increase in the number of spines and in the number of multiple-synapse boutons (where multiple spines contact the same presynaptic bouton). (Lamprecht and LeDoux, 2004)

1.5.4 RNA binding proteins and synaptic plasticity

Cognitive function and memory rely on synaptic plasticity, the ability of synapses to modify their strength in response to stimulation. Emerging evidence indicates that posttranscriptional gene regulation is necessary for synaptic plasticity at several levels: by increasing proteome diversity through alternative splicing, or by enabling activity-dependent regulation of mRNA localization, translation or degradation in the dendrite. All

of these steps are regulated by different RNA binding proteins suggesting an involvement in this process. To date, three RNA-binding proteins have been found to play crucial roles in different types of synaptic plasticity: FMRP for mGluR-dependent LTD (Huber et al., 2002, Koekkoek et al., 2005), CPEB for NMDA-dependent LTP of EPSCs (Si et al., 2003), and Nova for NMDA-dependent LTP of sIPSCs (Huang et al., 2005).

FMRP, CPEB and Nova2 null mice have defects in specific aspects of synaptic plasticity (fig.3). Hippocampal mGluR-dependent LTD is enhanced in knockout mice lacking the Fragile X mental retardation-1 gene (Fmr1) (Huber et al., 2002). In tissue culture cells, stimulation of mGluRs results in localization of Fmr1 mRNA into dendrites (Antar et al., 2004) and rapid translation of FMRP in synaptosomes (Weiler et al., 2004). In contrast to FMRP, which appears to mediate translational inhibition, CPEB functions by relieving translational inhibition (Huang et al., 2002). A link between CPEB and the regulation of LTP was suggested by the finding that CPEB is activated by Aurora and CaMKII-mediated phosphorylation following NMDA stimulation in primary neurons and synaptosomes (Huang et al., 2002). Surprisingly, studies of CPEB-1 KO mice revealed a defect in early LTP (E-LTP), but not in the protein synthesis-dependent phase of LTP (Late LTP) (Alarcon et al., 2004). CPEB stimulates polyadenylation of a large pool of synaptic RNAs (Du and Richter, 2005) and might also regulate CaMKII a and MAP2 mRNA dendritic localization (Huang et al., 2005). These studies suggest that the link between the regulation of RNA localization and the regulation of local translation at the synapse might generally be mediated by RNA-binding proteins such as ZBP1, FMRP and CPEB.

The increasing interest in the role of RBP in synaptic plasticity was confirmed by a new paper of Zhang G. (Zhang et al.) in witch was showed the accumulation of RNA binding protein at postsynaptic density during the synaptic activity. Zhang G. identified activity-dependent modifications in the composition of postsynaptic densities (PSDs) isolated from rat primary neuronal cultures.

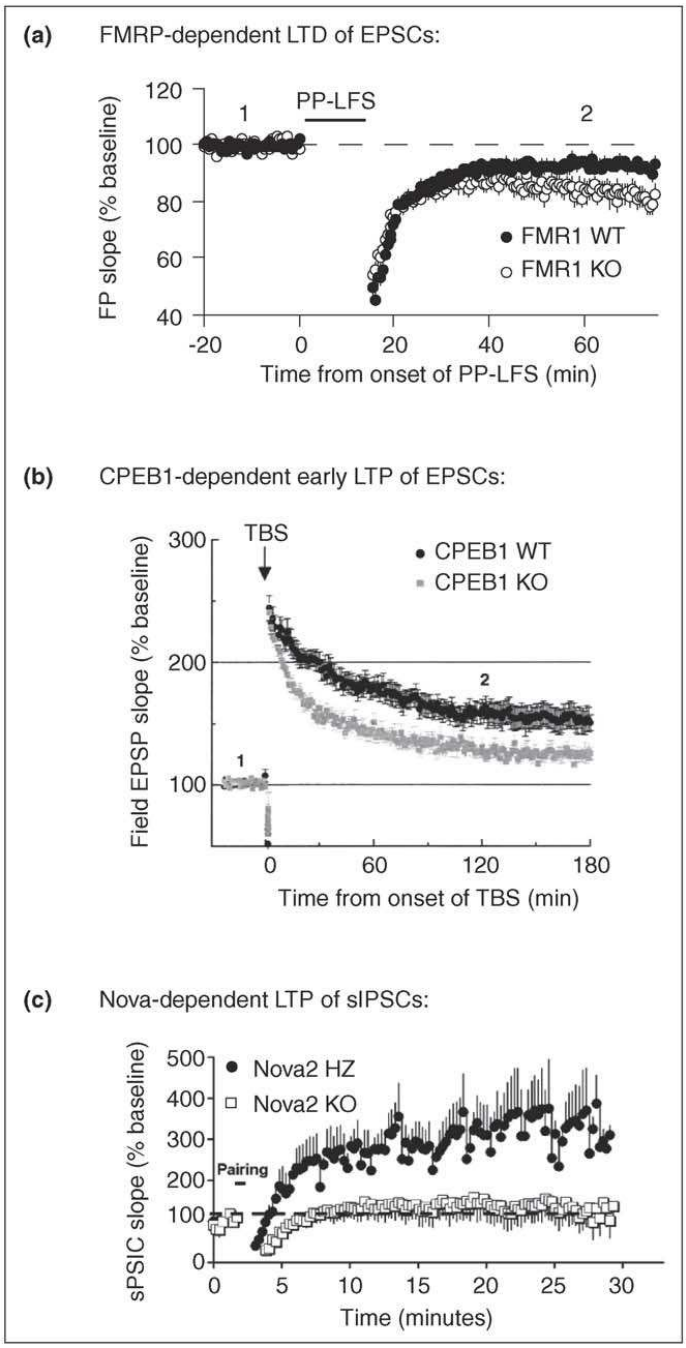

Fig. 12 FMRP, CPEB and Nova2 null mice have defects in specific aspects of synaptic plasticity. (a) Synaptic induction of mGluR-LTDusing paired-pulse low frequency stimulation (PP-LFS) repeated at 1 Hz for 15 min is significantly enhanced in hippocampus of Fmr1-KO mice as compared with that in wild type (WT) controls.(b) LTP evoked by one train of theta burst stimulation is significantly decreased in hippocampus of CPEB-1 KOs as compared with that in WT controls. (c) Pairing-induced activation of NMDA-R potentiated slow inhibitory postsynaptic currents (sIPSC) in the hippocampus of a Nova-2 heterozygote, but not Nova-2 knockout mice.

He found that synaptic activity resulted in increased abundance of diverse RNABPs, including heterogeneous nuclear ribonucleoproteins (hnRNPs) A, A2/B1, A3, M, D, G, and L. In fact, 12 of the 37 proteins whose expression were altered in the PSD were RNABPs, suggesting that neuronal activity regulates synaptic RNA metabolism. Moreover Zhang G. found that knockdown of hnRNP M and hnRNP G, but not hnRNP A2/B1 or hnRNP D, resulted in marked changes in dendritic spine density. These results suggest a crucial role for hnRNP proteins in synaptic function and provide support for the notion that local regulation of RNA metabolism underlies the synapse-specific and activity-dependent regulation of dendritic spine morphology (Zhang et al.).

1.5.5 Arp2/3 complex and N-WASP in synaptic plasticity

It is already known that both N-WASP and Arp2/3 complex are implicated in synaptic plasticity. In fact many paper demonstated their involvement in change in the number, size, and shape of dendritic spines that is associated with synaptic plasticity, which underlies cognitive functions such as learning and memory. This plasticity is attributed to reorganization of actin, but the molecular signals that regulate this process are poorly understood. The knockdown of endogenous N-WASP expression by RNA interference or inhibition of its activity by treatment with a specific inhibitor, wiskostatin, caused a significant decrease in the number of spines and excitatory synapses. Deletion of the C-terminal VCA region of N-WASP, which binds and activates Arp2/3 complex, dramatically decreased the number of spines and synapses, suggesting activation of the Arp2/3 complex is critical for spine and synapse formation. Consistent with this, Arp3, like N-WASP, was enriched in spines and excitatory synapses and knock down of Arp3 expression impaired spine and synapse formation. A similar defect in spine and synapse formation was observed when expression of an N-WASP activator, Cdc42, was knocked down (Wegner et al., 2008). Thus, activation of N-WASP and, subsequently, the Arp2/3 complex appears to be an important molecular signal for regulating spines and synapses. Arp2/3-mediated branching of actin could be a mechanism by which dendritic spine heads enlarge and subsequently mature.

2 AIM OF THE WORK

Emerging evidence indicates that postranscriptional gene regulation is necessary for synaptic plasticity at several levels: by increasing proteome diversity through alternative splicing, or by enabling activity-dependent regulation of mRNA localization, translation or degradation in the dendrite. Each of these steps is regulated by specific RBPs. A recent study found 380 putative RBPs in the mouse genome, 237 of which were detected in brain, and 16 of which showed neuron-specific expression (McKee et al., 2005).

hnRNP K is a nuclear riboprotein highly expressed in embryonic and adult brain with a noteworthy enrichment in the cortex and hippocampus (Blanchette et al., 2006). Recently work demonstrated the interaction of hnRNP K with Abelson-interacting protein 1 (Abi-1) in postsynaptic sites and hypothesized possible involvement in spine morphology (Proepper et al.) strongly suggesting that hnRNP K may have a fundamental neuronal function; this idea is in agreement with a new paper about the accumulation of RBP proteins at the postsynaptic density during synaptic activity. In fact. Zhang demonstrated that synaptic activity induces an increase in diverse RNA binding proteins included the heterogeneous nuclear riboproteins (hnRNPs) G, A2/B1, M and D (Zhang et al.).

The main aim of this project was the characterization of hnRNP K function in neuron.
We focused our attention on two different sides: first of all we analyzed role of hnRNP K on neuron morphology, subsequently on synaptic function.
At this purpose, we investigated the effect of hnRNP K loss in rat hippocampal pydamidal neurons. We analyzed hnRNP K knockdown on dendritic arborization, dendritic spines (density and morphology) and excitatory synapse with special attention on pre- and post-synaptic compartments.
The target of the second part of our study was to look how hnRNP K influences neuronal function. We quantified the miniature postsynaptic currents (mEPSCs) in basal condition and subsequently after cLTP induction. Given the effect of hnRNP K loss in synaptic transmission, we studied its role in this phenomenon by analysis of expression changes of hnRNP K and its localization during the cLTP.

In the last part of this project we are investigating the possible mechanism underlying all of this phenotypes inducted by the absence of hnRNP K.

This study may be considerable for the understanding the role of RBP protein in neuronal function with special attention to synaptic plasticity to improve our knowledge about learning and memory.

3 MATERIALS AND METHODS

3.1 DNA CONSTRUCTS

Full length ha-hnRNP K were a gift from Yoo Y (Yoo et al., 2006).
The 21 base pair target sequence that was used to design hnRNP K small interference RNA is the following: GGAACAAGCCTTTAAAAGA. The siRNA is specific only for the rat sequance. siRNA- hnRNP K was subcloned in GFP pll3.7 siRNA and GFP pLVTM siRNA.

3.2 NEURONAL CULTURES AND TRANSFECTION

Primary hippocampal neurons were prepared from embryonic days 18–19 rat brains (Brewer et al., 1993) and placed on coverslips coated with poly-D-lysine (30 µg/ml) and laminin (2 µg/ml) at a density of 75,000/well for immunocytochemistry, and at 300,000/well for biochemistry experiments.
The cultures were transfected using the calcium phosphate method at DIV (Day In Vitro) 7or 12 and fixed at DIV 14 or 20 (as indicated in results).

3.3 IMMUNOCYTOCHEMISTRY

Hippocampal neurons were fixed in 4% paraformaldeyde- 4% sucrose for 10 minutes at room temperature or cold methanol for 8 min at -20°C and incubated with **rabbit anti**: -HA (1:200, Santa Cruz Biotechnology Inc.), -VGAT (1:400, Synaptic System), -VGLUT (1:400, Synaptic System), or with **mouse anti**: -GluR2 (1:100, Chemicon), -HA (1:200, Roche Applied Science), -hnRNP K (1:100, Santa Cruz Biotechnology Inc.), -PSD-95 (1:100, NeuroMab), GDB1X solution (2X: gelatin 2%, Triton X100 10%, 0.2M Na_2HPO_4 pH 7.4, 4M NaCl) for 2 hours at room temperature.
Cells were then washed and incubated with Cyanine 3 or Cyanine 5 (1:200, Jackson Laboratories) conjugated secondary antibodies diluted in GDB1X solution for 1 hour at room temperature.

3.4 TIME-LAPSE IMAGING

Neurons on coverslips were transferred to a stage chamber and imaged at 37℃ using a LSM 510 Meta confocal microscope, with 63x objective and 4x zoom, with and average of 2 scans. Neurons were imaged for 40 minutes, taking images at 5 min intervals. At each time point, 0.75 µm Z stacks of images were collected. To evaluate spine turnover we compared images at time 0 with those at time 40, counting the numbers spines that appeared and disappeared over this period.

3.5 IMAGE ACQUISITION AND QUANTIFICATION

Confocal images were obtained using a Nikon 60x objective with sequential acquisition setting at 1024x1024 pixels resolution. Each image was a 'z' series projection of approximately 5 to 7 images taken at 0.75 µm depth intervals. Transfected neurons were chosen randomly for quantification from two to five coverslips from three to five independent experiments. Morphometric measurements were performed using MetaMorph images analysis software (Universal Imaging, West Chester, PA). The analysis of dendritic arborization was done by using a procedure according to the Sholl's method (Sholl, 1953). Concentric rings (10 µm between rings) were placed over pictures of neurons and the number of intersections of the dendrites with the concentric rings were counted. Dendritic spine number and size were quantified using Metamorph image analysis software (Universal Imaging Corporation) as described (Passafaro et al., 2003).
Fuorescence intensity measurements were performed using Imagej images analysis software.

3.6 STATISTICAL ANALYSIS

All data were analysed with an unpaired Student's *t*-test and ANOVA oneway. Asterisk symbols in the figure indicate significant differences at *P<0.05, **P<0.01 and ***P<0.001, respectively.

3.7 CO-IMMUNOPRECIPITATION

Hippocampus and cortex from rat adult brain was homegenated in ice cold Lysis Buffer (PBS, 1% CHAPS, EDTA pH8 0.1mM, protease inhibitor cocktail). Lysates were centrifugated at 13200rpm for 20min at 4℃ and supernatants were incubated at 4℃ with Protein A-agarose beads (Santa Cruz, CA, U SA) conjugated with rabbit IgG (5µg/ml SIGMA). Beads were discharged by centrifugation and clarified supernatants were incubated at 4℃ with Protein-A beads conjugat ed with anti-hnRNP K (5µg/ml MBL Inc.) or IgG rabbit (5µg/ml) as control for 4 hours or overnight. Beads were then collected by centrifugation, washed three times with lysis buffer and two times with PBS plus protease inhibitors and, after resuspension in sample buffer and boiling for 5 minutes, analyzed by SDS-PAGE.

3.8 SDS PAGE, WESTERN BLOT ANALYSIS

Proteins were separated in 10% SDS-PAGE and electroblotted onto nitrocellulose membranes in buffer containing 0.025 M Tris-HCl, 0.192 M glycine, 20% methanol, pH 8.3 at 240 mA for 120 min. The reactions were performed by incubating with primary the antibodies (RT, 2-3h in 4% milk): -**rabbit abs anti** hnRNP K (1:1000 MBL), N-WASP (1:200, Santa Cruz Biotechnology Inc.), GluR1 (1:1000, Chemicon), GluR2/3 (1:500, was a gift from Gotti C.), GAPDH (1:1000, Santa Cruz Biotechnology Inc.), **-mouse abs anti** Tubulin (1:1000, Sigma), GFP (1:1000, Roche Applied Science), PICK1 (1:500, NeuroMab), NR1 glutamate receptor (1:1000, Pharmigen), synapsin (1:2000 Synaptic System) and synaptophins(1:1000, SIGMA). Horseradish peroxidase-conjugated anti-rabbit or anti-mouse secondary antibodies (1:4000 GE Healtcare) were used as secondary antibodies (RT, 1h in 3% milk). Immunoreactive bands were visualized by enhanced chemiluminescence (ECL, GE Healtcare).

3.9 LENTIVIRAL PRODUCTION AND INFECTION

Lentiviruses expressing GFP or hnRNP K-siRNA were produced using HEK293T FT cells as described by Lois et al. (2002).
Hippocampal neurons were infected at DIV8 with hnRNP K-siRNA or GFP and used at DIV14.

3.10 ELECTROPHYSIOLOGICAL RECORDINGS

Hippocampal pyramidal neurons were plated on 16mm glass coverslips, at an average density of 150 000/coverslip. After 14-15 days in vitro, the coverslips were transferred to a chamber at the input stage of an upright microscope (NIKON Eclipse FN1) and perfused with the following extracellular solution (mM): NaCl (140), KCl (3), CaCl2 (2), MgCl2 (1.2), glucose (10), hepes (10); adjusted to pH 7.4 with NaOH. Recording temperature was set at 28-30°C, through a feedback device (TC324B-Warner Instruments). Patch pipettes were filled with the following solution (mM): K-gluconate (126), NaCl (4), hepes (10), glucose (10), MgSO4 (1), CaCl2 (0.5), EGTA (1), ATP-Mg (3), GTP-Na (0.1); pH adjusted to 7.2 with KOH. In this condition, the free-calcium concentration estimated in the solution is around 100nM.
Whole-cell patch-clamp recordings were obtained by conventional methods (Hamill et al, 1981). Post-synaptic currents were acquired using a Multiclamp 700B ampilfier (Axon Instruments-Molecular Devices), digitized through a Digidata 1440A (Axon Instruments-Molecular-Devices), visualized online and recorded using the pClamp10.2 software (Axon Instruments-Molecular Devices). After 2 minutes after assessing the whole-cell configuration, mEPSCs were recorded in presence of 3□M TTX (Tocris), filtered at 2kHz and digitized at 20kHz using Clampex 10.2 software. A 10-15 minutes period was adopted to evaluate mean mEPSCs amplitude and coefficient of variation (CV = standard deviation/mean amplitude); longer periods usually did not improve the estimates.
All signals were digitally lowpassed at 1.5kHz before offline analysis, performed using Clampfit 10.2 software.

Miniature currents were detected setting a proper threshold (5pA) from the baseline. nonNMDA-mediated mEPSCs were recorded at a holding potential of -70mV, at which the NMDA current is blocked by Mg^{2+} (signals were completely blocked by perfusion of 10μM of the nonNMDARs blocker CNQX, data not shown). The NMDA component of mEPSCs was evident at the holding potential of +60mV and can be separated from the nonNMDA component. For the analysis of mEPSCs recorded at +60mV, the peak of the nonNMDA component is measured using a 1ms window centered on the time of the peak of the response at -70mV (recorded in the same cell). The measurement of the NMDA component was considered as the average current in a 10ms window, centered 35ms after the start of the signal rising phase.
nonNMDA mEPSCs kinetics were measured at -70mV, where the NMDA component was absent. The signal decay was fitted with a double exponential function:

(1) $y(t)=A1\ exp^{-t/\tau 1} + A2\ exp^{-t/\tau 2}$

NMDA mEPSC kinetics were measured at +60mV, where the NMDA component is well separated from the nonNMDA component. NMDA decay was measured starting 35 msec after the signal starting point and NMDA current decay was fitted according to equation 1. The weighted decay time constant (Rumbaugh and Vicini, 1999) for the NMDA current was estimated as:
$\tau w= \tau 1 \bullet [A1/(A1+A2)]+ \tau 2 \bullet [A2/(A1+A2)]$.

Series resistance (Rs) was monitored throughout the recordings; accepted deviation in this parameter recorded over the time window used for statistical analysis was <10%. Rs was compensated of 20-60%, and was always <10Mμ
For every neuron recorded, principal passive parameters (Cm, Rm, Rs) were calculated and did not statistically differ among the conditions tested.
A 10-15 minutes period was adopted to evaluate mean mEPSCs amplitude and coefficient of variation (CV = standard deviation/mean amplitude); longer periods usually did not improve the estimates.
Results are reported as mean±MSE (mean standard error) and, unless otherwise indicated, statistical comparisons are done using Student's t test (statistical significance for $p<0.05$).
All drugs were obtained from Sigma Aldrich, unless otherwise stated.

3.11 CHEMICAL LTP

For cLTP experiments, the extracellular solution used was a normal ACSF (nACSF) with the same composition described above and with in addition (μM): 20 bicuculline, 3 strychnine, 3 TTX.
The intrapipette solution was the same described above. Neurons were maintained in the nACSF for at least ten minutes of recording; then the LTP-ACSF solution was perfused for 3 minutes, before switching again to the nACSF for the rest of the experiment. The LTP-ACSF had the same composition as the normal extracellular solution described above but without Mg2+, and the addition of (μM): 200 glycine, 20 bicuculline, 3 strychnine.
This protocol has been described in literature to induce a chemical form of long term potentiation (cLTP), that is NMDA-dependent (Lu et al., 2001).

3.12 ISOLATION OF CREDE SYNAPTOSOME/FRACTIONATION OF BRAIN TISSUE

Three week-old high-density cultures of rat hippocampal neurons or fresh tail of rat brain were homogenized using cold homgenization buffer (0.32 M sucrose, 10mM HEPES pH7.4, 2 mM EDTA, protease inhibitors and phosphatase inhibitors as below) and spined at 1000g for 15 min to separate pelletd nuclear fraction (P1).
The supernatant (S1) was recovered and centrifuged at 10.000 g to produce a crude synaptosomal pellet (P2) and a supernatant (S2) which contains the cytosol and the light membranes. all of these fractions were also assessed by immunoblotting analysis.

4 RESULTS

4.1 hnRNP K LOCALIZATION IN NEURON AND BRAIN

Previous studies demonstrated the presence of hnRNP K mRNA and protein in the rat nervous system during the embryo development. The expression level gradually decreases during development until it is rescricted to a very limited number of structures including the hippocampus and some regions of the cortex.

We confirmed this decrease by biochemical experiments using brains from adult and embryo rats. We analyzed the expression of hnRNP K in total brain and we observed a reduction of hnRNP K in adult rat compared with embryo (fig. 1A).

Subsequently we analyzed the localization of endogenous (fig1A right panel) and overexpressed hnRNP K (fig. 1B) in culture of hippocampal neurons. Using an immunocytochemistry assay we observed that the protein mainly localizes in the nucleus but is detectable also in soma and dendrites. The localization of hnRNP K protein in different cellular compartments is consistent with the presence of nuclear shuttling domain (KNS).

To better investigate hnRNP K subcellular localization we extracted the proteins from total rat brain following a special protocol that allows to separate different cellular fractions: nuclear fraction (P1), cytoplasmic fraction (S1), crude synaptosomal fraction (P2) and light membranes (S2) (fig. 1C).

We observed an enrichment of hnRNP K in P1, interestingly it was also detectable in crude synaptosomal fraction (P2) and in the other fractions (S1 and S2).

4.2 hnRNP K KNOCK-DOWN CAUSES MORPHOLOGICAL ALTERATIONS IN YOUNG AND MATURE HIPPOCAMPAL NEURONS

To study a possible role of hnRNP K in neuron we designed a small interference RNA able to silence the endogenous protein in rat and we cloned it in GFP pll3.7 and GFP pLVTHM vectors.

A

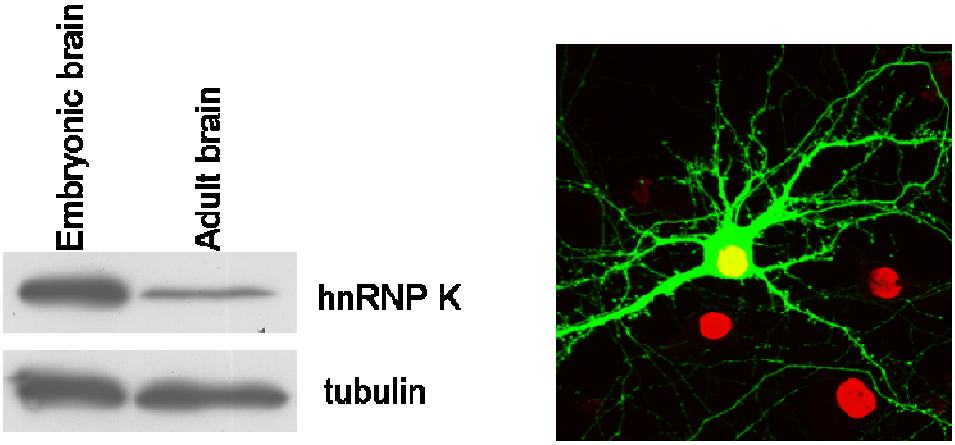

B

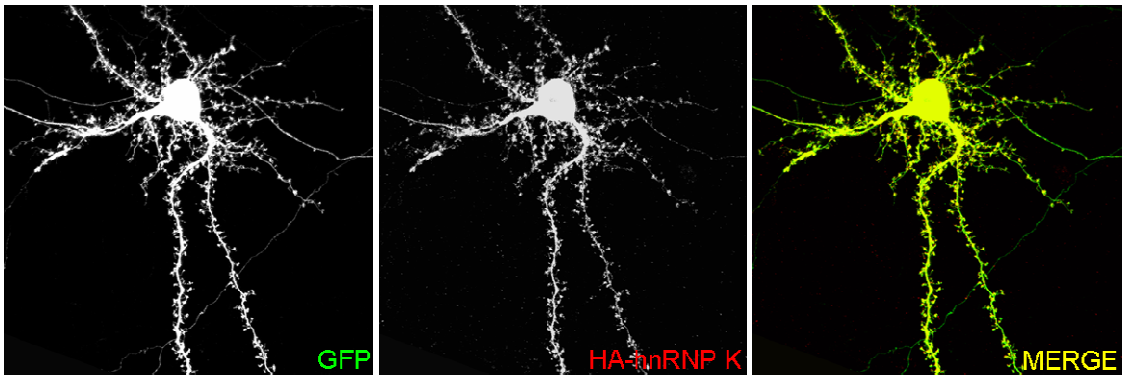

C

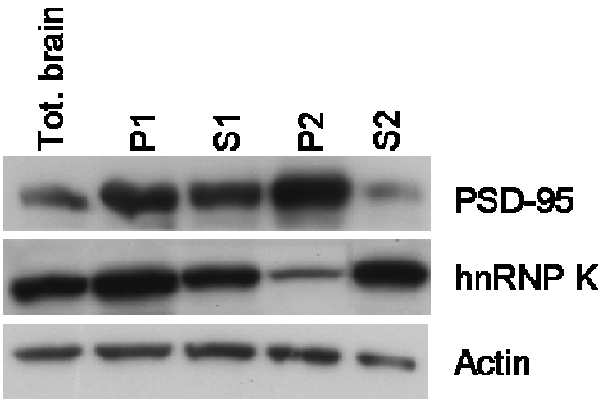

Fig.1 Expression and localization of hnRNP K protein. **(A)** Different level of hnRNP K expression in adult rat brain compared with embryo (left panel) endogenous localization in mature neurons at DIV 20 (right panel); **(B)** Localization of overexpressed protein, in mature neurons.; **(C)** Localization of endogenous protein in different subcellular fractions.

To test the efficacy of siRNA we infected rat hippocampal neurons at DIV8 using lentiviruses expressing siRNA- hnRNP K or scrambled as control.
After 7 days, the infection by lentiviruses expressing siRNA reduced significantly the level of hnRNP K expression compared to control (Fig.2A).

A

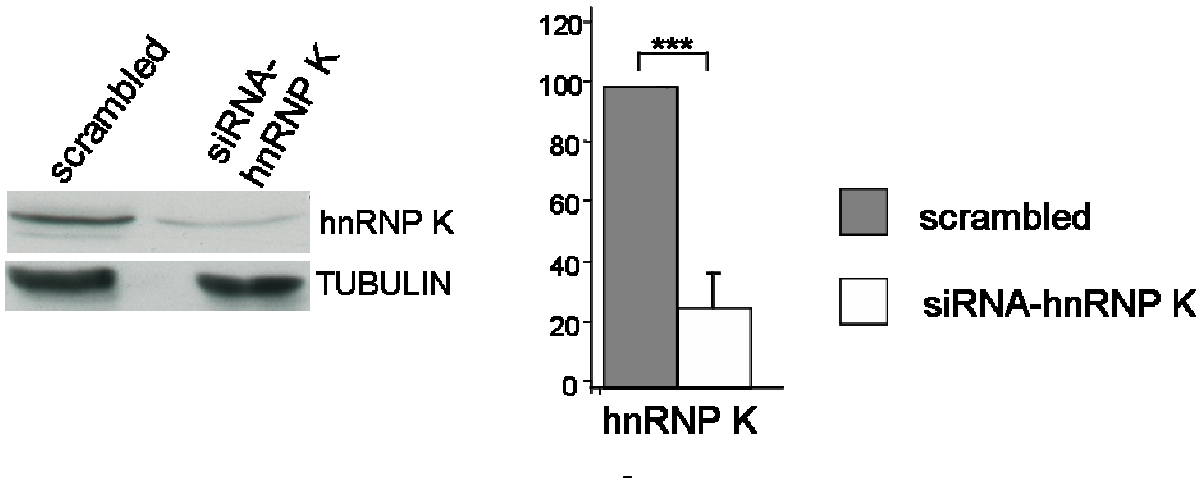

Fig. 2 (A) Validation of siRNA-hnRNP K in rat hippocampal neurons infected altenativily with scrambled or siRNA-hnRNP K.

4.2.1 The silencing of hnRNP K expression causes a decrease in the number of dendrites

We transfected immature (DIV7) hippocampal neurons with siRNA-hnRNP K or scrambled to investigate if the knock-down of hnRNP K leads to any alteration in neuronal morphology and we fixed them one week after (fig 3A). We observed a significant reduction in the number of dendrites evaluated by Sholl analysis (fig 3B). To demonstrate the specificity of siRNA we cotransfected a siRNA-resistant construct without the target sequence recognized by hnRNP K-siRNA. The rescue constract was able to rescue this phenotype.

A

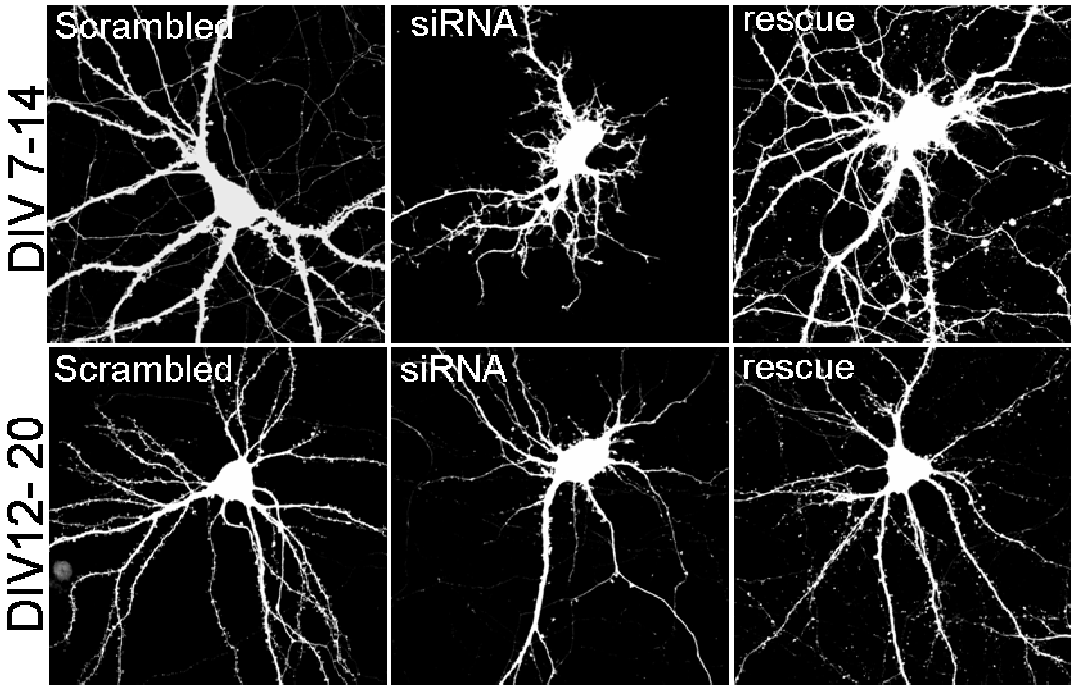

B

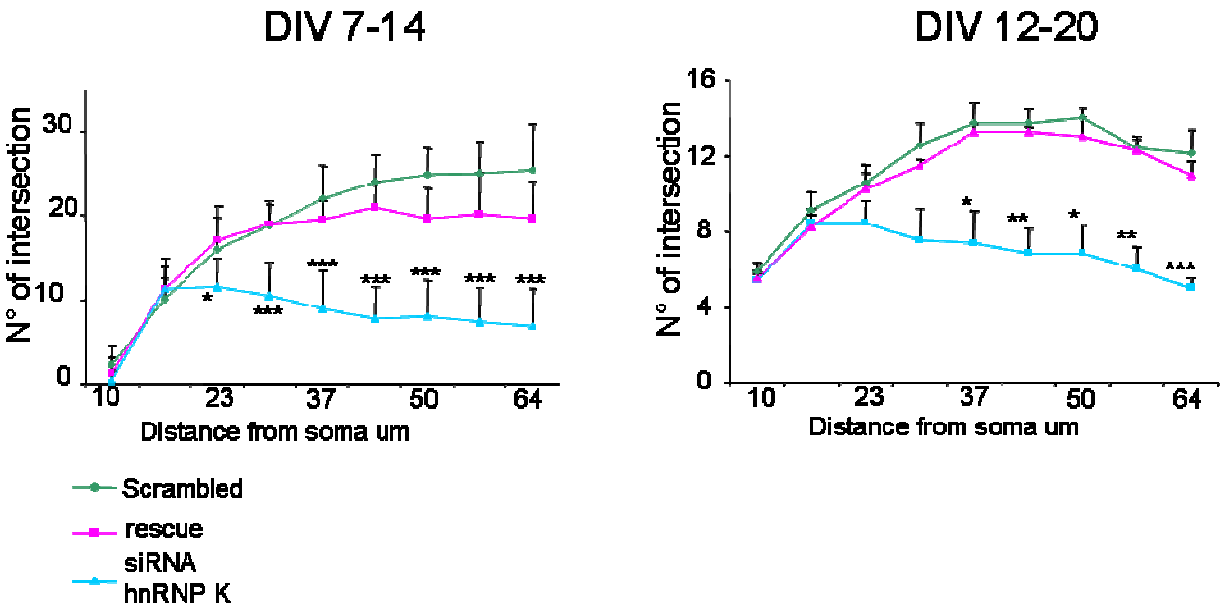

Fig. 3 (A) In rat hippocampal neurons transfected at DIV7 and fixed at DIV14, the knockdown of hnRNP K expression causes a reduction in the number of dendrites compared with controls and rescue neurons. **(B)** quantification of dendrites number performed by Sholl analysis.

A

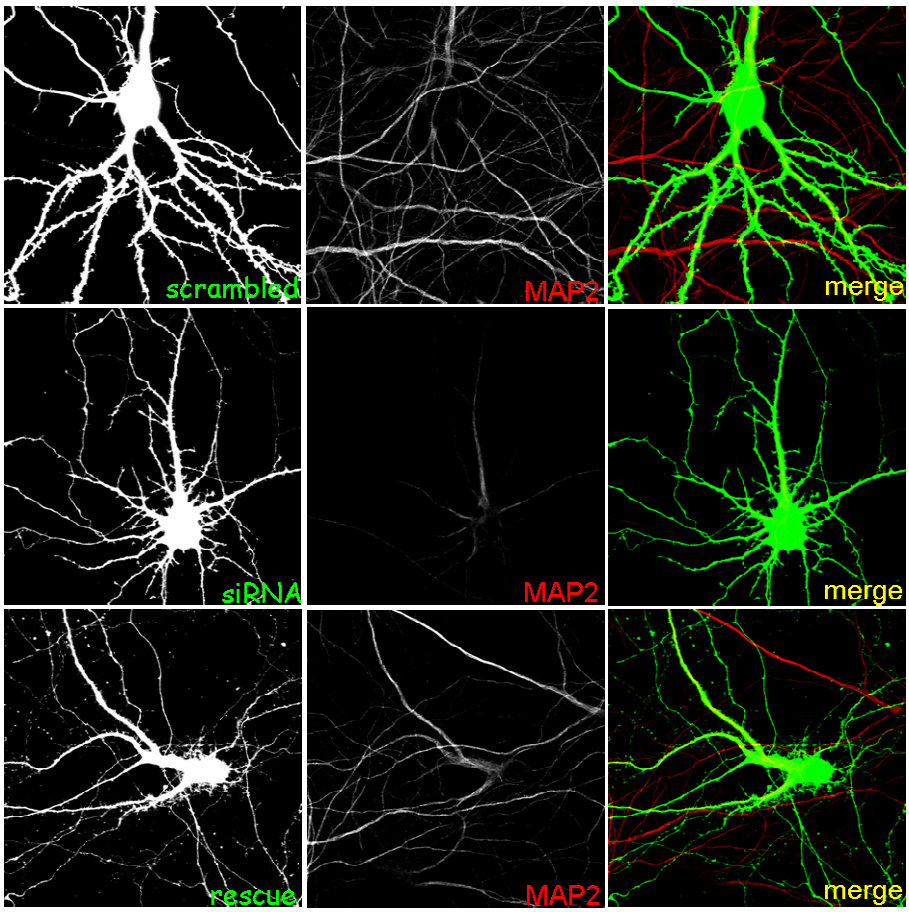

B

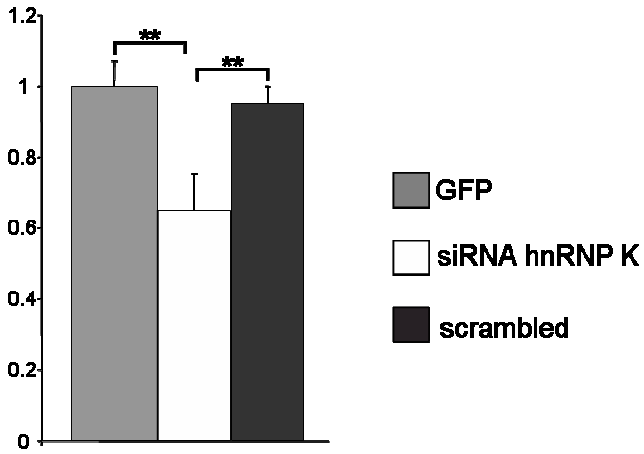

Fig. 4 (A) Immunostaining for MAP2; the dendritic alterations in neurons expressing hnRNP K siRNA are associated with a decrease in MAP2 staining; this decrease is rescued by cotransfection with siRNA-resistant wild-type hnRNPk contruct. **(B)** Quantification of integrated intensity of MAP2 performed by using of Imagej software.

Moreover we observed the same reduction in the number of dendrites silencing mature neurons (DIV12) and also in this case the rescue of phenotype was possible.
Then, to verify if also the structure of dendrites was altered we performed an immunostaining experiments for MAP2 protein (fig. 4A); the level of MAP2 protein expression was significantly reduced in neurons transfected with siRNA- hnRNP K compared to control (1±0.07 vs 0.65±0.1; $p<0.01$) and rescue (0.95 ±0.05 vs 0.65 ± 0.1; $p<0.01$) (Fig. 4B).
This data suggest an involvement of hnRNP K in dendrites development and maintaining.

4.2.2 Knock-down of hnRNP K alters spine morphology and turnover.

We transfected mature hippocampal neurons (DIV12) with GFP or hnRNP K-siRNA and we analyzed spine density and morphology using Metamorph image analysis software at DIV20 (fig. 5A).
We found that the absence of hnRNP K induced a reduction in spine density compared to control and rescue neurons. Indeed the neurons transfected with scrambled showed 4.59±0.26 spines per 10 μm of dendrite, while neurons transfected with siRNA- hnRNP K 3.01±0.32 spines in 10 μm ($p=0,002$). The reduction in spine density was rescued by coexpression of hnRNP K resistant construct (5.11± 0.56 $p=0.005$) (Fig.5B).
Unexpectedly spine shape was unaffected and the measurement of spine length and width not show any change (Fig.5B).
Subsequently we focused our attention on spine stability and turnover. To this purpose we performed time laps imaging experiments. Neurons were transfected at DIV 12 alternatively with siRNA-hnRNP K or scrambled as control and the imaging experiments were performed at DIV20.
Neurons were imaged for 40 minutes, and the images were taken every 10 min (Fig. 6A). We observed an increase in spine turnover in silenced neurons: the percentage of new spines appeared and lost spine disappeared during 40 min was higher in knockdown neurons compared to control (Fig. 6B).

A

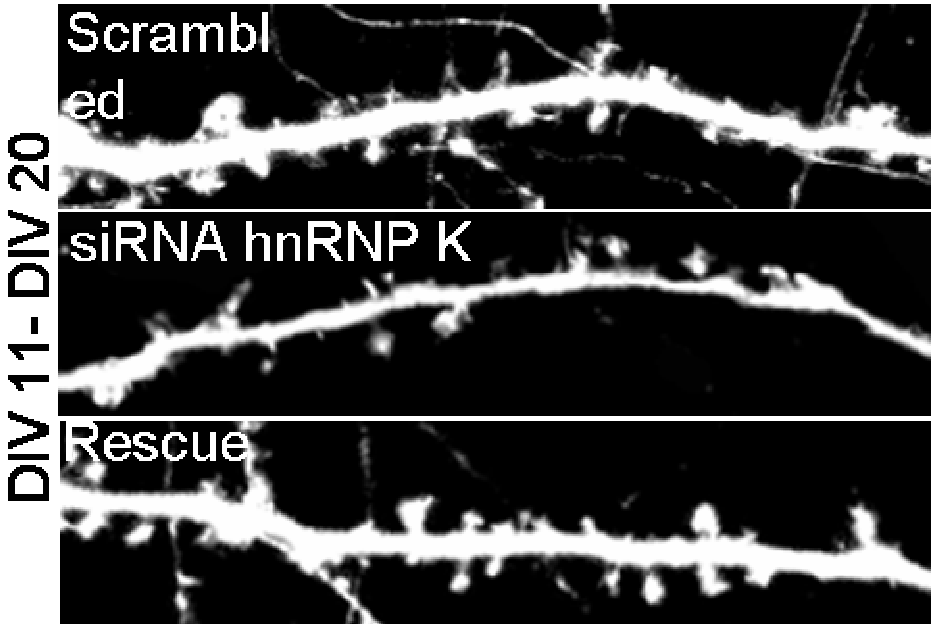

B

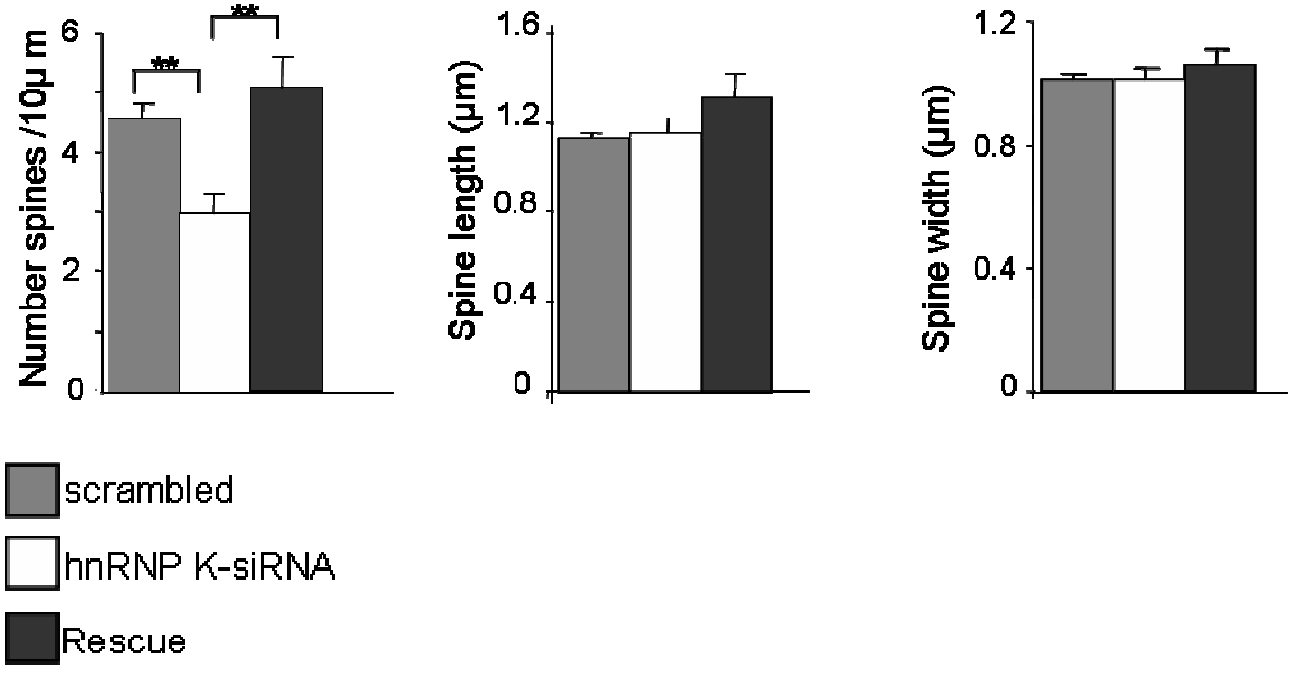

Fig. 5 (A) Dendrites from Neurons overexpressing alternatively scrambled-siRNA-hnRNP K, siRNA-hnRNP K or Rescue. **(B)** Neurons overexpressing siRNA-hnRNP K have the same spine length and width but reduced spine density ($p<0,01$) than control neurons; this effect is rescued by cotransfection with siRNA-resistant wild-type construct.

A

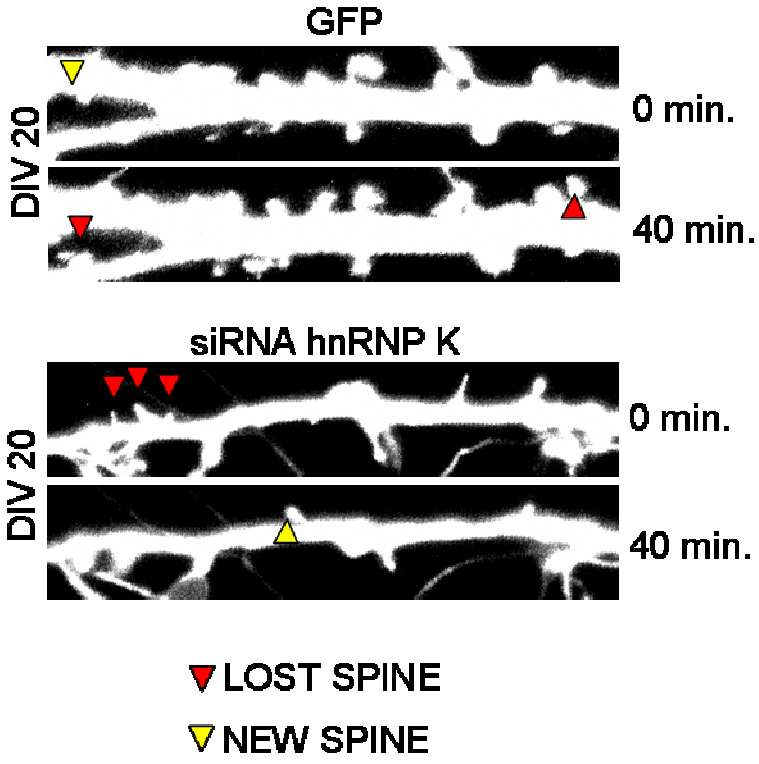

B

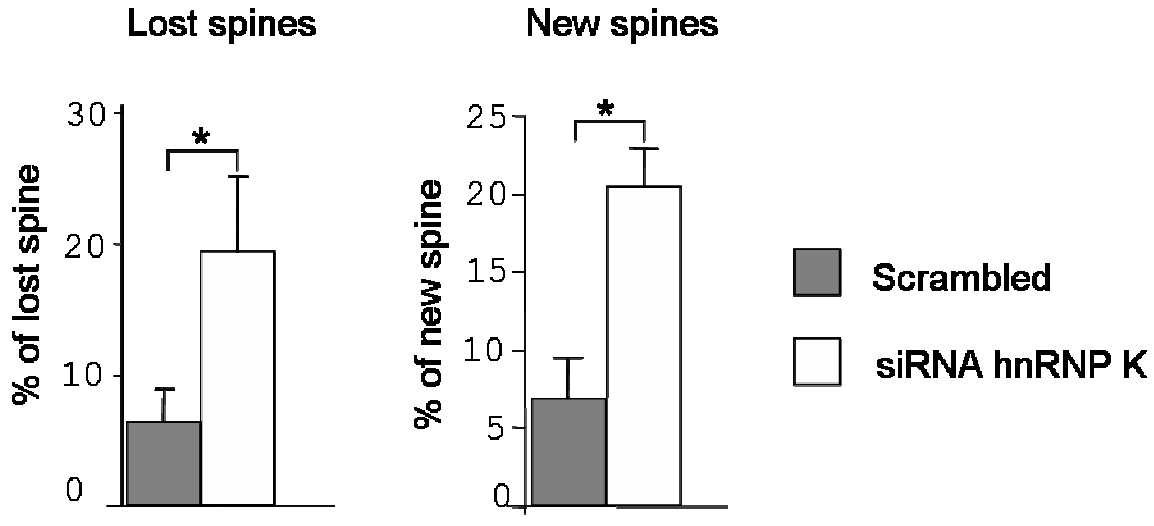

Fig. 6 (A) In vivo imaging of neurons (DIV20). **(B)** In neurons that express hnRNP K siRNA there are a significant increase in the spine turn over.

4.3 hnRNP K AND THE EXCITATORY SYNAPSE

4.3.1 Lost of hnRNP K induces a reduction in the level of postsynaptic markers

Given these alterations in spines, we subsequently focused on the asset of synaptic proteins. In particular, we performed immunocytochemical experiments on hippocampal neurons using different antibodies to characterize the effect of hnRNP K absence on synaptic markers.

Neurons were transfected at DIV7 and DIV12 with siRNA- hnRNP K or scrambled as control and we quantified the level of pre- and postsynaptic markers at DIV14 (data not shown, but in agreement with the results obtained with neurons at DIV20) and DIV20 (fig. 7A).

The quantification showed a significant reduction in the staining intensity of postsynaptic markers GluA2 (1±0.14 vs 0.42±0.08, **$p<0.01$) and PSD-95 (1±0.13 vs 0.37±0.08, **$p<0.01$) in neurons expressing hnRNP K-siRNA compared to control neurons (fig. 7B).

By contrast the staining intensity of presynaptic markers VGAT and VGLUT did not change (VGLUT 1±0.05 vs 0.82±0.12, $p>0.05$ and VGAT 1±0.04 vs 0.88 ±0.04, $p>0.05$) (fig. 7B).

In order to confirm these results by biochemical experiments we used Hek FT cells to produce lentiviruses able to infect cultures of neurons to increase to knockdown effect.

The viral particles expressing alternatively GFP or hnRNP K-siRNA were used to infect hippocampal neurons at DIV8. The neurons were solubilized one week after the infection and different samples were loaded on acrilamide gel (Fig. 8A).

We analyzed different pre- and postsynaptic markes and as expected we observed a reduction only in PSD-95 and GluR2, while presynaptic markers synapsin and synaptotagmin and other synaptic proteins like PICK1 were unaffected (fig. 8B).

Unexpectedly the level of AMPA subunit GluR1 and NMDA subunit NR1 did not show any change (fig. 8B).

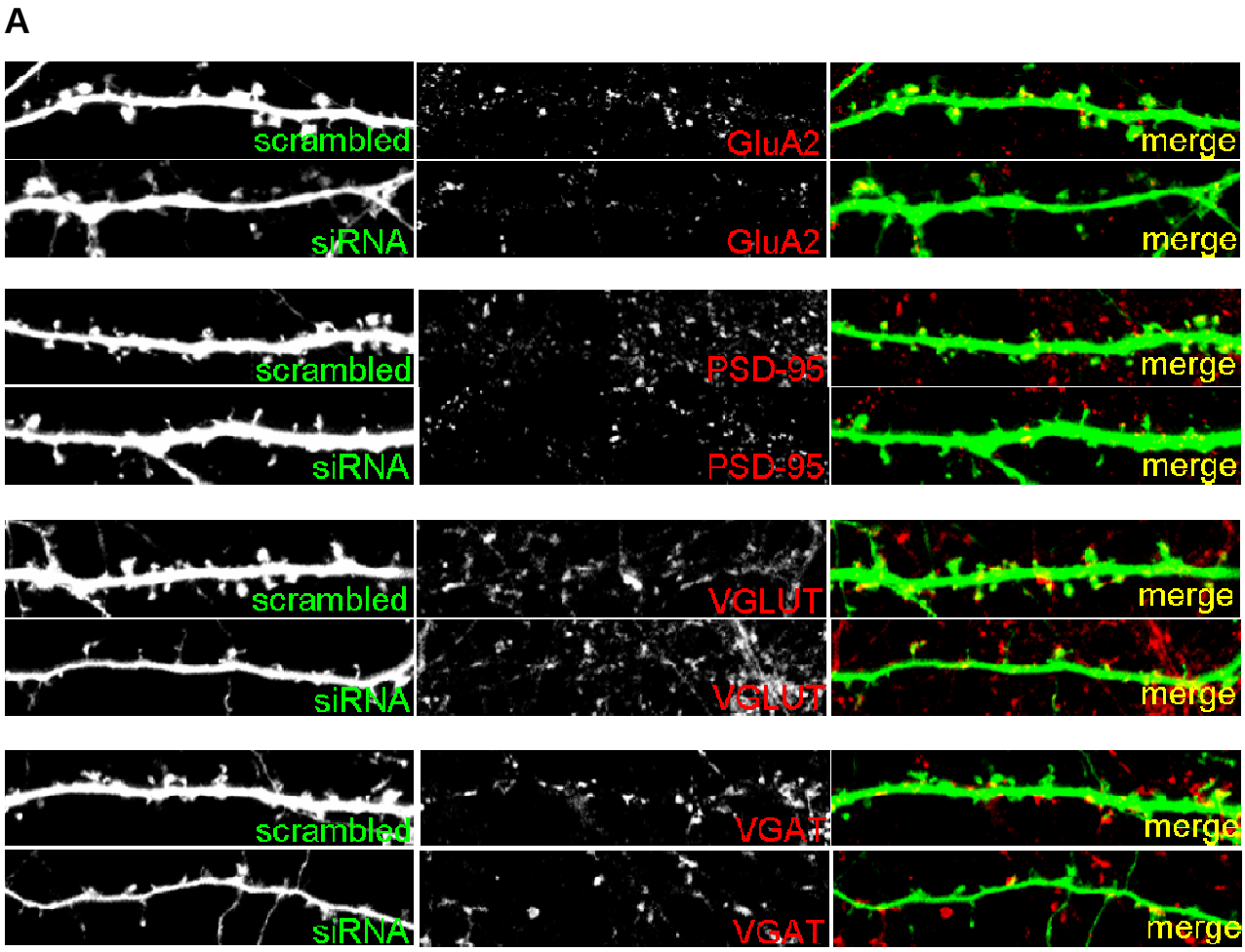

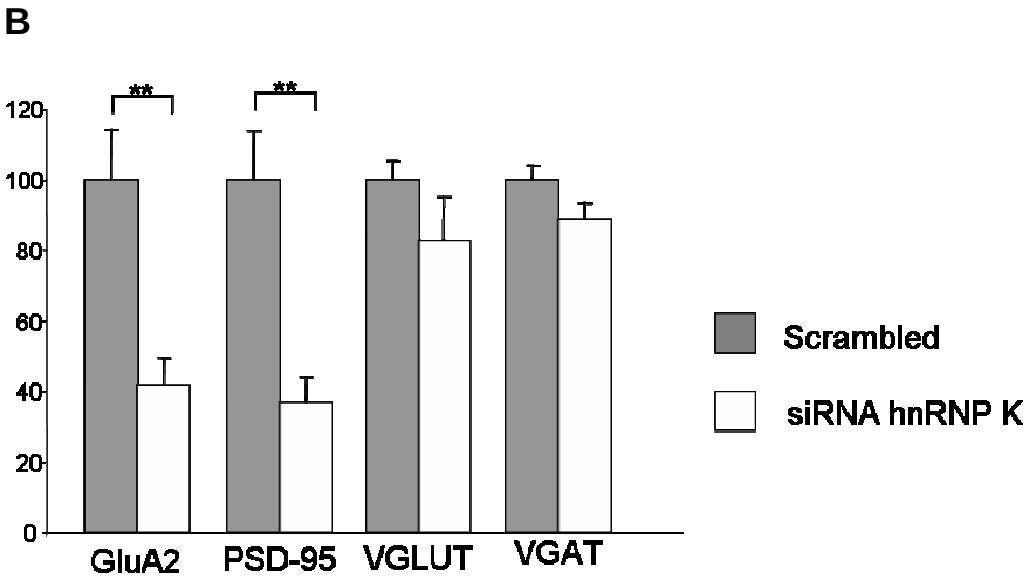

Fig.7 Quantification of synaptic markers expression. **(A)** Immunostaining for endogenous PSD-95, GluA2, VGLUT and VGATin neurons at DIV20 transfected at DIV12 with scrambled or siRNA-hnRNP K. **(B)** Quantification of the synaptic proteins fluorescence intensity performed by using of IMAGEJ analysis software.

A

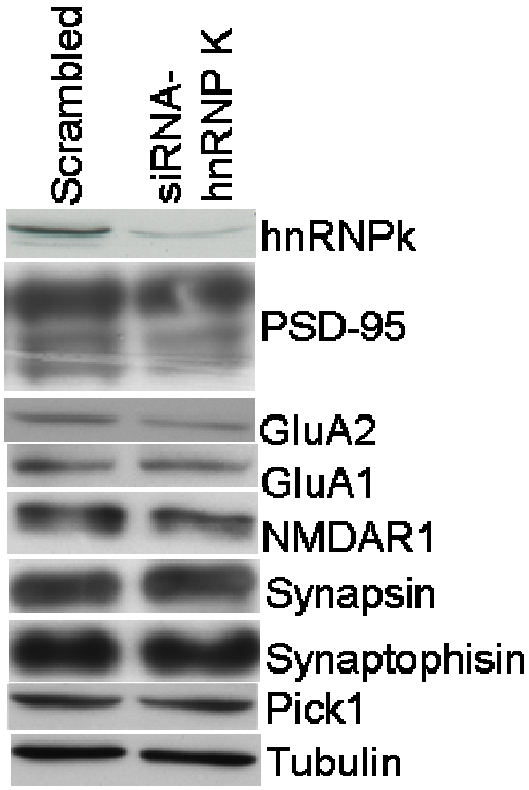

B

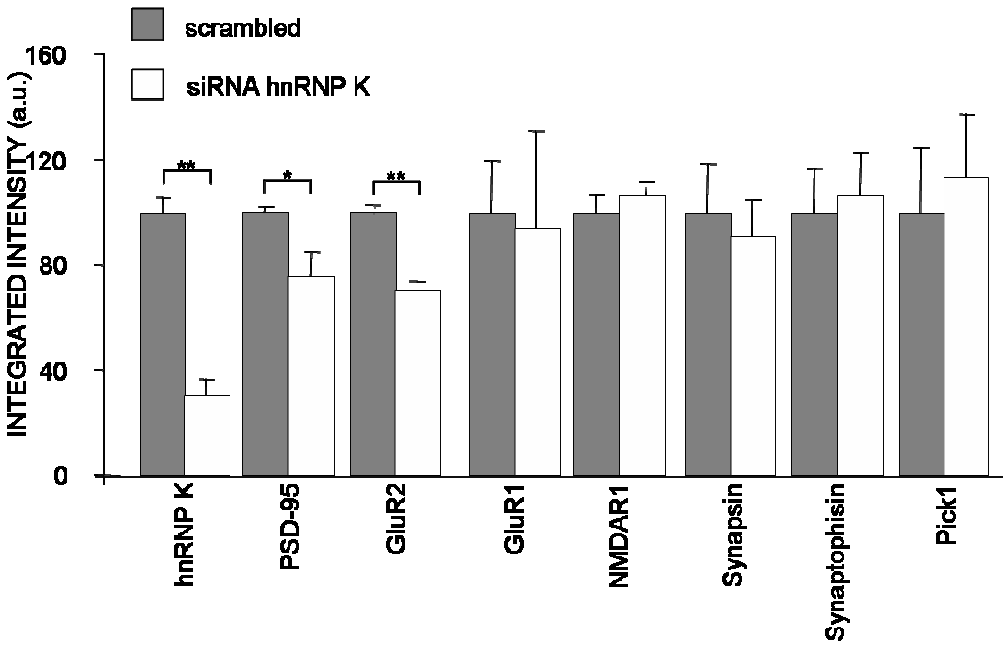

Fig.8 Quantification of synaptic markers expression. **(A)** Immunoblotting from neurons infected by lentiviral vector; The neurons were infected at DIV8 by lentivirus expressing siRNA or scrambled and lysated at DIV13. **(B)** Quantification of the synaptic proteins expression performed by using of IIMAGEJ software.

4.3.2 hnRNP K knock down impairs the excitatory synapse morphology and function

Given these strong effects of hnRNP K loss in postsynaptic compartment, we next examined the excitatory synapse. To this purpose we quantified the puncta area of excitatory postsynaptic merker PSD-95 and excitatory presynaptic merker VGLUT and area of their co-localization.

Hippocampal neurons were infected at DIV8 by lentiviruses expressing hnRNP K-siRNA or scrambled as control. At DIV18 we performed immunostaining for PSD-95 and VGLUT to analyze the shape of excitatory synapse and its pre- and postsynaptic compartment. Compared to neurons expressing scrambled, silenced neurons had significantly smaller clusters for PSD-95 (1±0.04 vs 0.72±0.04, ***$p<0.001$), but not for VGLUT (1±0.05 vs 0.9±0.06, $p>0.05$) .

This result Is consistent with the decrease in postsynaptic markers only, found in immunostaining experiments.

As expected the loss of hnRNP K induced changes also in the co-localization area between PSD-95 and VGLUT (1±0.03 vs 0.78±0.04, **$p<0.01$). Taken together these findings show that hnRNP K is required for the maturation of postsynaptic compartment, by contrast it is not necessary for spine shape.

Subsequently we investigated if these alterations in synapse were linked to impairments in synapse function by study miniature postsynaptic currents.

Electrophysiological recordings were performed on DIV15-16 primary hippocampal neurons, transfected with GFP-expressing scramble and siRNA for hnRNPK. Excitatory, AMPAR-mediated, transmission was taken into account. Miniature postsynaptic currents (mEPSCs) were unveiled at -70mV(holding potential) by the presence of 3μM TTX in the bulk perfusion. Currents were completely inhibited by CNQX perfusion (data not shown). These AMPAR-mediated mEPSCs were analyzed for current peak amplitude and average frequency. Our results showed that, while no significant difference was detected for peak amplitude (-20.7±2.2 pA and -20.8±2.8 pA, respectively; $n=8$ for both conditions, t test N.S.), miniature currents frequency was dramatically decreased in silenced neurons (from 2.4±0.6 Hz in scramble to 0.7±0.2 Hz in silenced neurons; $n=8$, $p<0.01$). The co-tranfection of a siRNA-resistant hnRNPK construct allowed the rescue of this effect in

A

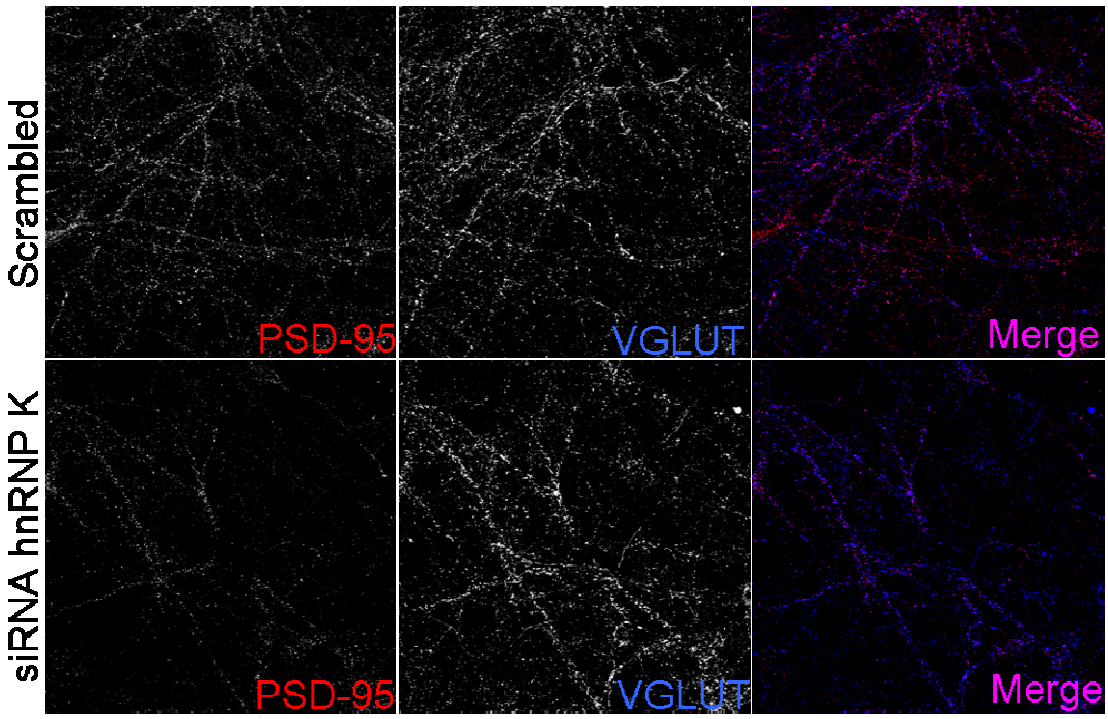

B

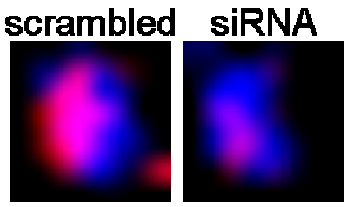

C

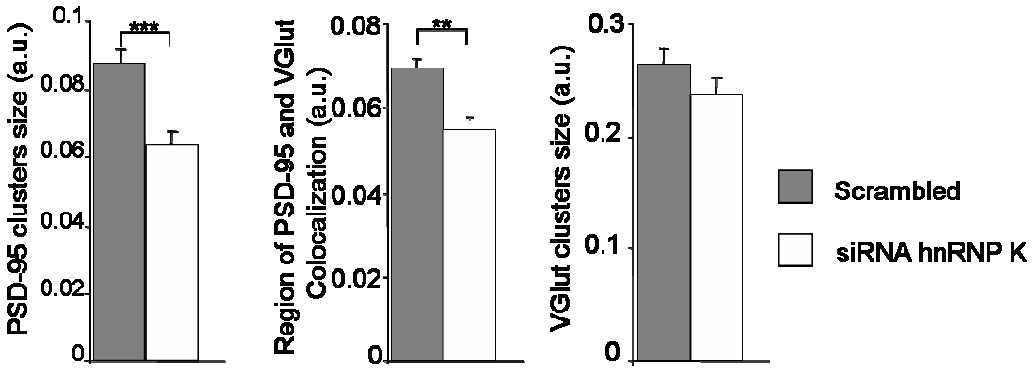

Fig.9 (A) Neurons infected by lentivirus vector expressing scrambled or siRNA hnRNP K. The staining for PSD-95 and VGLUT shows, in silenced neurons, a reduction of size of PSD-95 clusters and **(B)** of the region of PSD-95 and VGlut colocalization. **(C)** Quantifications performed by using of IIMAGEJ software.

A

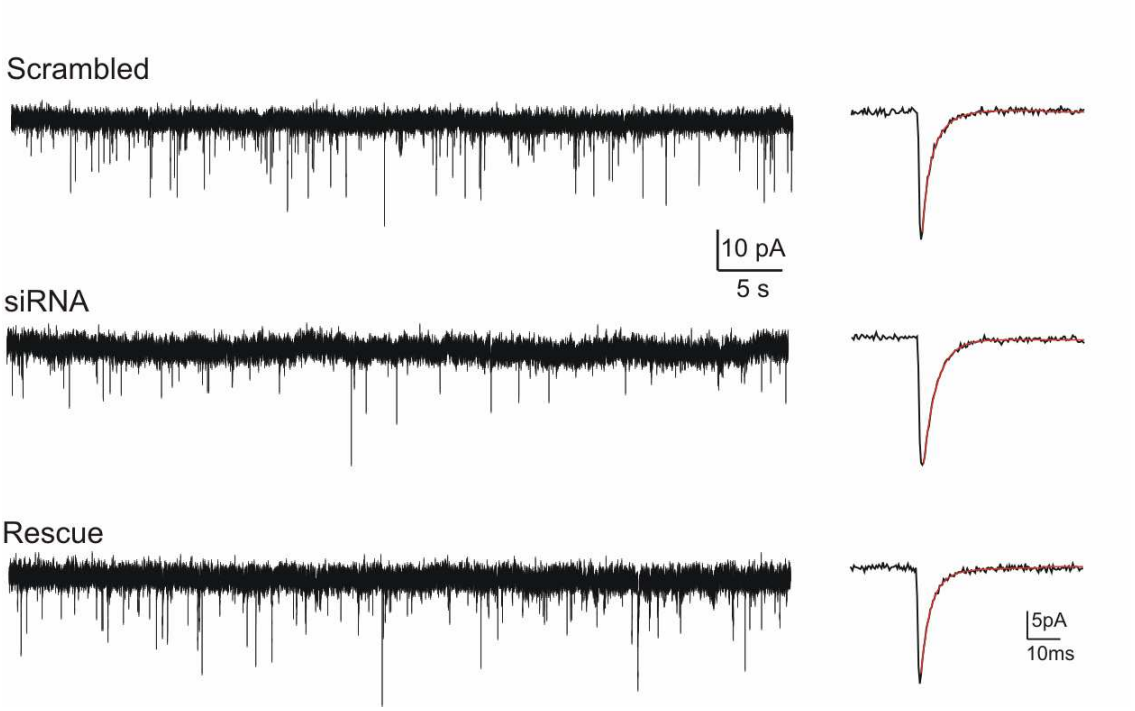

B

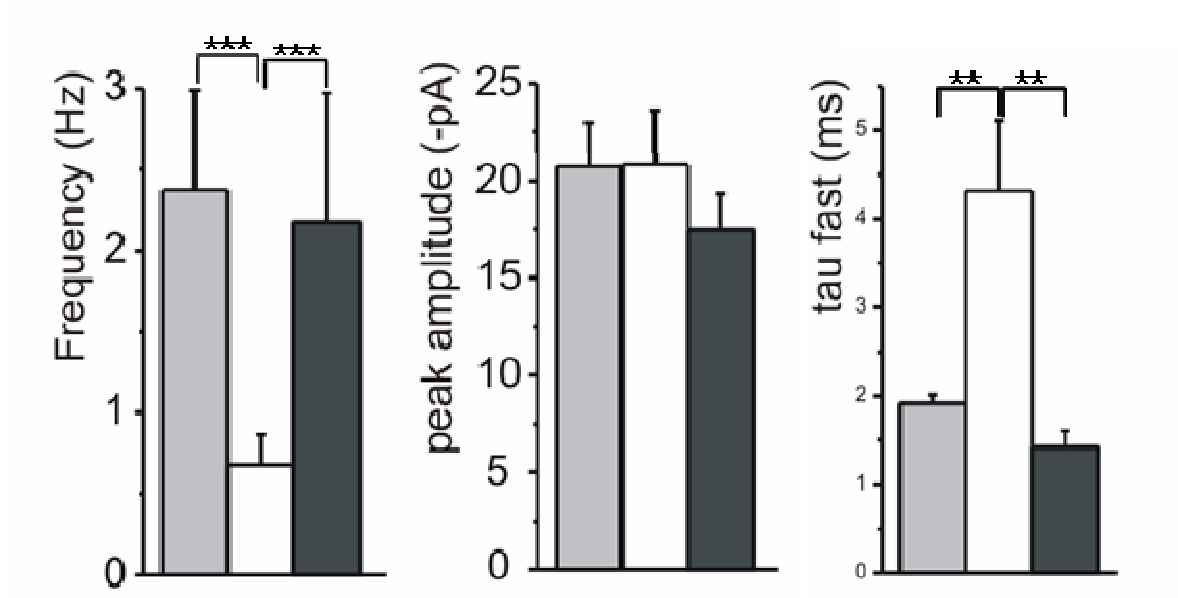

Fig.10 (A) Miniature excitatory postsynaptic currents (mEPSCs) recorded from transfected neurons (1min traces). To be noted the decrease in currents frequency in hnRNP K silenced neurons; mEPSC peak amplitude did not change. These results are summarized in the histograms in A1. (B) Averages of 50 mEPSCs for the three conditions tested. The currents decay is slower in recordings from silenced neurons. The histogram in B1 shows the average values of the fast component of the biexponential decay .

siRNA transfected cells. Indeed, in these latter experiments, no significant change was found in peak amplitude (-17.4±1.8 pA; n=10, t test N.S. vs both scramble and siRNA alone); mEPSCs frequency was similar to that detected in scrambled neurons (2.2±0.8 Hz; n=10, t test N.S. vs scramble; $p<0.01$ vs siRNA alone). The lower mEPSC frequency is well explained by the decrease in dendritic spines number in silenced neurons. Since the size of spines head is correlated to the quantity of AMPARs exposed in the membrane, the absence of a change in mEPSCs amplitude is in agreement with the results previously shown (no change in spine size).

Interestingly, a further analysis of these currents revealed a change in the decay kinetic. In particular, mEPSCs decay was fitted using a biexponential equation (see Methods), that provided a quantification of the slow and the fast component of current decay. The fitting was applied to an average trace of 100 mEPSCs per neuron. The fast component of the decay (tau-fast) was increased in silenced neurons, respect to scramble and rescued conditions (4.32±0.79ms vs 1.92±0.09 and 1.42±0.18 ms, respectively; n=8,8,10; $p<0.01$ siRNA vs both scramble and rescue). These results indicate that miniature currents decay is slower in silenced neurons. The decay of AMPARs currents is determined by the receptor subunit composition (Jonas, 2000), that confers slower or faster gating kinetics. In hippocampal CA1 pyramidal neurons, AMPARs are composed for the 81% to GluA1A2 heteromers (Lu et al., 2009). In particular, Lu and collaborators showed that GluA1 and GluA2 subunit manipulations revealed that when GluA2 subunit is lacking, homomers of GluA1 subunits produce signals with slower decay kinetics, respect to that originated from GluA1A2 heteromers. This is in good agreement with our previous results (a decrease in total GluA2, no change in GluA1, in siRNA vs scramble transfected neurons).

These data describe a strong impairment of excitatory neurotransmission. This suggests that signals integration and information processing in a network made of neurons lacking hnRNP K should be deeply affected.

4.4 hnRNP K IN SYNAPTIC PLASTYCITY

4.4.1 Chemical LTP induction is impaired in hnRNP K silenced neurons

In order to investigate this aspect, a chemical form of LTP has been induced in culture of hippocampal neurons at DIV14-15. In particular, after ten minutes of mEPSCs stable recording, 200μM glycine (and 3μM strychnine, see methods for details) was perfused for 3 minutes (Lu et al., 2001). Miniature currents were then recorded for 40 minutes after glycine perfusion. In scrambled neurons, mEPSCs peak amplitude increased after cLTP induction in a significant manner, as expected (+28±6%, at 5min after glycine perfusion; n=7, $p<0.0005$). This increase was maintained for all the duration of recordings. Similarly, mEPSCs frequency increased of 33±5% (n=7, $p<0.01$) and coefficient of variation decreased from 0.44±0.05 to 0.31±0.04 after cLTP induction (same n, $p<0.002$). These results suggest a role of the presynaptic compartment in cLTP induction, in good agreement with previously reported literature (Citri and Malenka, 2008). When the same cLTP induction protocol was applied to neurons silenced for hnRNP K, the current amplitude increase was not seen. Interestingly, miniature excitatory currents showed a decrease in amplitude that was statistically significant (-36±2%; n=8, $p<0.0001$), while no change in frequency or coefficient of variation was detected (-7±7% change in frequency, N.S.; CV varied from 0.55±0.04 to 0.52±0.04, t test N.S.). In those neurons in which the silencing of hnRNP K was accompanied with a cotransfection with the siRNA-resistant hnRNP K construct, all these impairments were rescued. More in detail, mEPSCs peak amplitude and frequency showed an increase, while CV decreased, not differently from what observed in scrambled neurons (peak amplitude +37±4%, n=8, $p<0.0001$; mean frequency +26±11%, $p<0.05$; CV from 0.38±0.04 to 0.31±0.03, $p<0.05$). If the cLTP induction protocol was not delivered, no significant change in mEPSCs peak amplitude was detected, in recordings that lasted 50-60 minutes, considering the three different experimental conditions tested /in Fig.X, the stability trace presented in the time-course graph refers to an average of the three single stabilities for scramble, silenced and rescued conditions.

The comparison of the three experimental conditions to the basal stability in absence of an induction stimulus, confirmed as expected the significance of the changes in peak amplitude described above (vs scramble $p<0.0000002$; vs silenced neurons $p<0.0002$; vs rescue $p<0.0000002$).

While the expression of this form of synaptic potentiation seems to involve the presynaptic terminal, the signals amplitude depression observed in silenced neurons, after the delivery of the same protocol that determines LTP in basal condition, seems to be due to the postsynaptic compartment, principally.

A

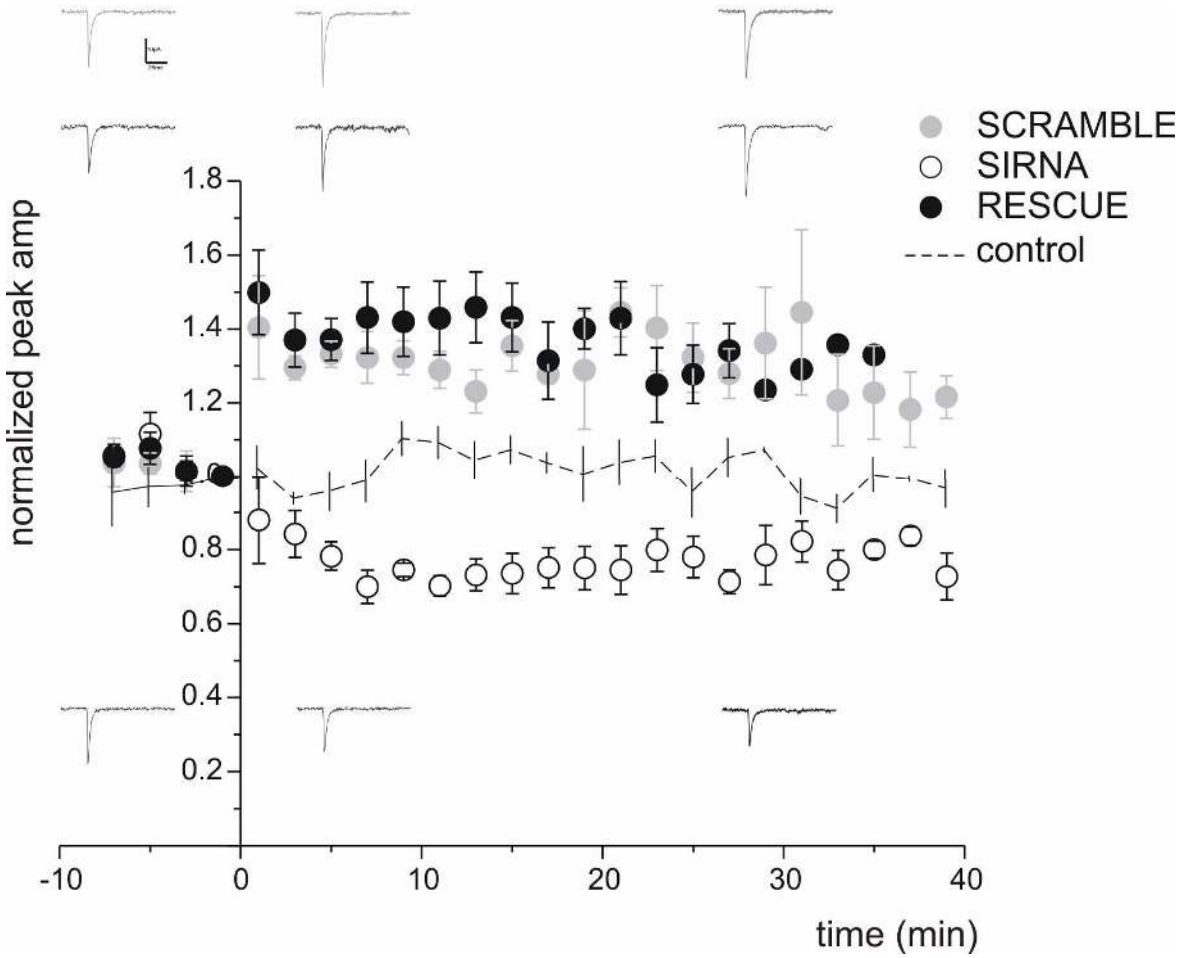

Fig.11 (A) cLTP induction is impaired in hnRNP K silenced neurons. At time 0, a cLTP induction protocol was applied. In silenced neurons mEPSCs amplitude did not increase after the induction, showing instead a statistically significant decrease. In the graph, currents peak amplitude is showed every 2 min and normalized for the value immediately before cLTP induction. At the top of the figure three averages of 50 single mEPSCs are reported, for siRNA-hnRNP K, Scrambled and Rescue, at -5', 5' and 30' after cLTP induction. The corresponding traces recorded from silenced neurons are reported at the bottom (scale bar 10pA/10ms).

In order to better understand the signals amplitude depression observed in silenced neurons we analyzed the synaptic compartments after cLTP induction. The neurons were infected at div 8 and treated at DIV 15 using exactly the same protocol as described for the electrophysiological experiments.

After 40 min an immunostaining for presynaptic marker VGLUT and postsynaptic marker PSD-95 was performed. In particular we analyzed the size of PSD-95 and VGLUT clusters and the size of co-localization region of both .

In fact it is already known that the LTP induces an accumulation of PSD-95 in spines and a consequently increase of co-localization region between pre- and post-synapse (Lu et al., 2001)

A

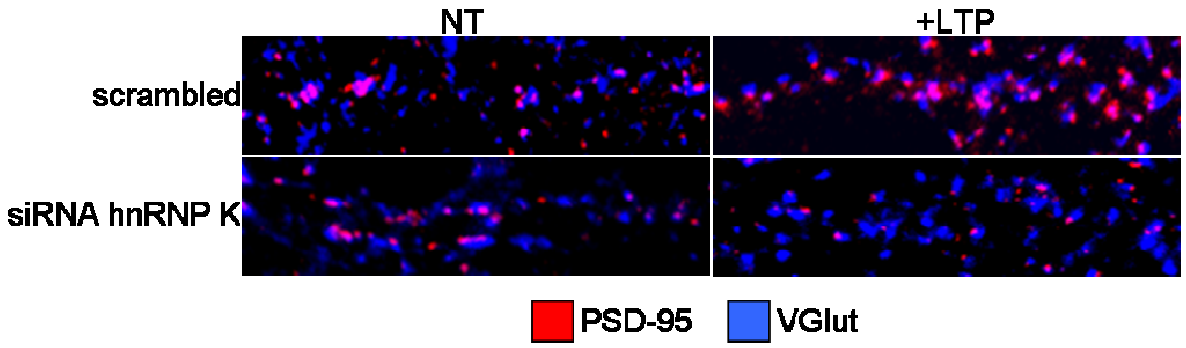

B

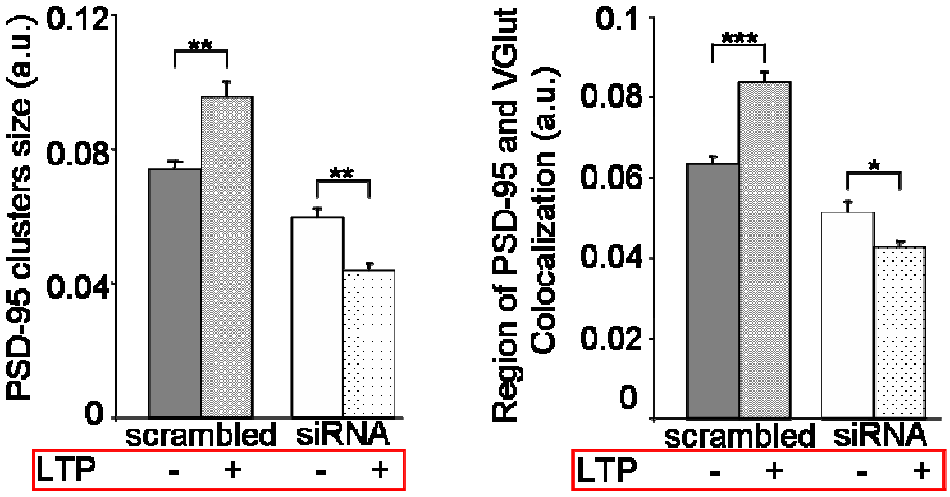

Fig.12 (A) Immunostaining for PSD-95 and VGLUT on neurons infected by lentivirus vector expressing scrambled or siRNA hnRNP K treated or not with glycine. **(B)** quantification of average size of PSD-95 clusters and average area of PSD-95 and VGLUT co-localization. The quantifications were performed by using of IIMAGEJ software.

As expected in scrambled neurons the treatment increased the size of PSD-95 clusters compared with untreated neurons (1±0.03 vs 1.28±0.06, **p<0.01) and the area of the co-localization region between PSD-95 and VGLUT (1±0.03 vs 1.32±0.04, ***p<0.001); by contrast, glycine treatment in silenced neurons induces a reduction of PSD-95 clusters compared with neurons not treated (1±0.05 vs 0.73±0.03, **p<0.01) and the size of the co-localization region between PSD-95 and VGLUT (1±0.06 vs 0.83±0.03, *p<0.05). No change was observed in the size of VGLUT (data not shown).

4.4.2 NMDAs in unaffected by hnRNP K silencing

The glycine-induced cLTP has been described to involve selectively the activation of NMDARs, as a necessary condition for the development of the AMPARs currents potentiation (Lu et al., 2001). A calcium-dependent switch between NMDA-dependent LTP and NMDA-dependent LTD has been described in hippocampus (Ref). In our experiments, it is likely that the synaptic depression observed after glycine perfusion in silenced neurons is due to a minor increase in calcium in the postsynaptic terminal, through the activation of NMDARs.

To check if this effect was caused by a lower number of NMDA receptor in synapse we decided to analyze NMDA component of glutamatergic response, at positive potentials.

The amplitude of NMDA component of the mEPSCs at +60mV (holding potential) was calculated as the average current in a 10 ms window centered on 35ms after the signal rise. At this time point, the AMPA component is completely decayed (as demonstrated by the AMPA current recorded at negative potentials, when NMDA component is blocked by Mg^{2+}). The average NMDA amplitude was similar in control and silenced neurons (20.4 ± 3.7 pA and 22.9 ± 4.2 pA, respectively; n=9 for both, t test N.S.). It has been described that the ratio between NMDA and AMPA component tends to be conserved in different conditions (Ref!). Therefore we checked the balance between these two components, calculating the peak of the AMPA component at +60mV as the average current in a 1ms window corresponding to the time of the current peak observed at -70mV. As expected, since mEPSCs amplitude at negative potentials did not change, the NMDA/AMPA ratio was not statistically different in GFP and silenced neurons, given a result of 0.75 ± 0.05 and 0.82 ± 0.4, respectively (n=9, t test N.S.). Given the differences in AMPA current

kinetics found in the previous analysis, mEPSCs decay at +60mV was fitted starting 35ms after the signal rise. No difference was found between scrambled and silenced signals.

A

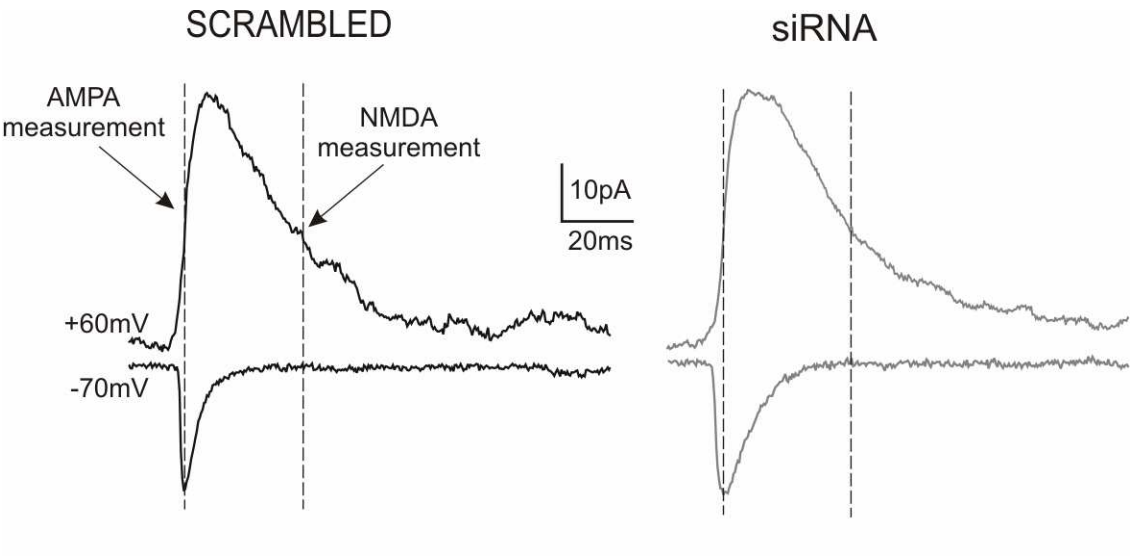

B

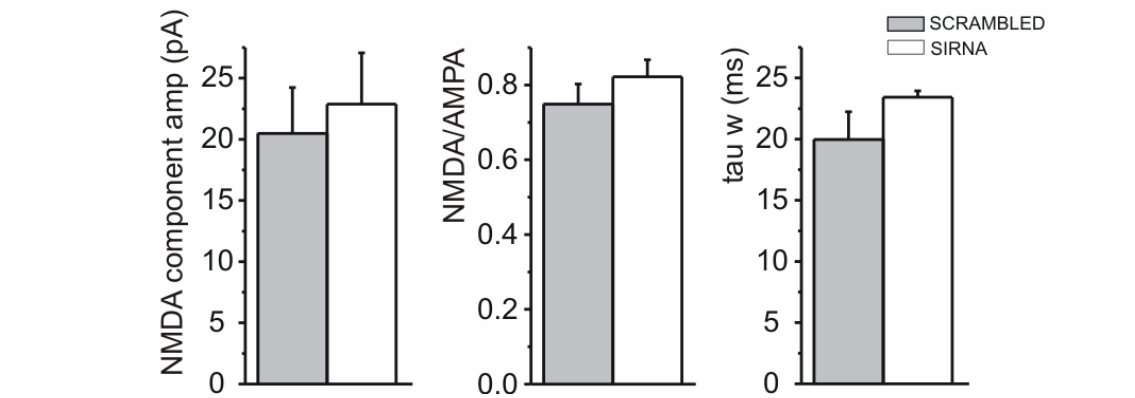

Fig.13 (A) NMDA component of mEPSCs in scambled and hnRNP K silenced neurons. Averages of ten single mEPSCs recorded at +60mV (to unravel the NMDA component) and at -70mV (pure AMPA component). Vertical dashed lines indicate at +60mV the region of AMPA measurement (in correspondence to the pure AMPA peak at -70mV) and NMDA measurement (35ms after signal rise, where pure AMPA component is absent). Traces from scrambled neurons in black (at left) and silenced neurons (at right). **(B)** Histograms show the values of NMDA component amplitude at +60mV, NMDA/AMPA ratio, and values of the kinetic parameter describing NMDA component decay phase (tau w).

4.4.3 cLTP induction leads to an increase of hnRNP K expression

Modulation of local protein synthesis in neurons plays a key role in the production of long-term, activity dependent changes in synapse structure and functional efficacy. Persistent form of synaptic change as seen in LTP and LTD typically requires rapid gene expression and new protein synthesis. By protein synthesis and degradation synaptic inputs may directly remodel the protein composition, and thereby the functional state, of individual dendritic spines or spine clusters.

Since in silenced neurons for hnRNP K, after the chemical LTP induction, the current amplitude increase was non observed, we further investigate if the protein could have a role in these phenomena. We analyzed the level of hnRNP K expression during LTP.

We quantified the amount of different proteins, including hnRNP K, at different time after the cLTP induction. In particular we analyzed: PSD-95, tubulin (as negative control) and hnRNP K. We quantified the level of proteins by western blott analysis using software IMAGEJ. All the values were normalized with the level of GAPDH.

We treated a different cultures of hippocampal neurons at DIV18 with glycine for 3 minutes and subsequently homgenated the neurons at different time after the treatment. The different time point were:

- t0= not treated,
- t1= 10 minutes after the treatment
- t2= 25 minutes after the treatment
- t3= 50 minutes after the treatment
- t4= 75 minutes after the treatment

As expected, the level of tubulin did not change after the cLTP induction (t0=1± 0.02; t1=0.88±0.03; t2=0.87±0.06; t3=0.92±0.01; t4=0.89±0.08). In the same way the total level of PSD-95 did not increase (t0=1± 0.001; t1=0.9±0.09; t2=1.11±0.05; t3=0.97±0.04; t4=1.16±0.06), in fact the long-term potentiation induces an increase of PSD-95 only in spines, but the total protein does not change (Kim et al., 2007). By contrast, we observed a strong increase of hnRNP K expression immediately after the treatment with glycine. We detected an higher level of hnRNP K jet 25 minutes after cLTP. The subsequent time points reconfirmed this increase (t0=1±0.01; t1=1.24±0.03; t2=1.82±0.23,**$p<0.01$; t3=1.75±0.1, *$p<0.05$; t4=1.87±0.13, **$p<0.01$;ANOVA oneway).

A

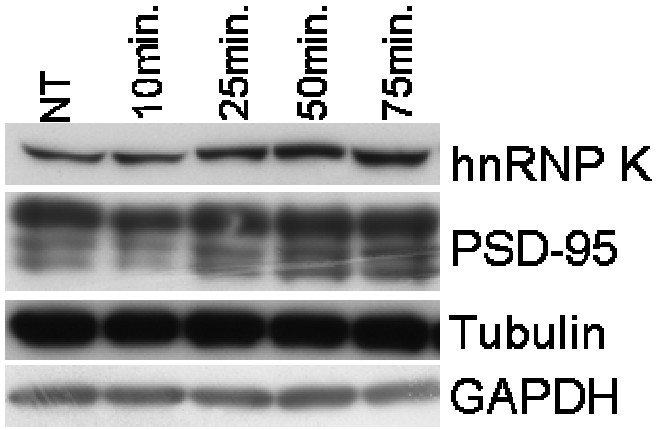

B

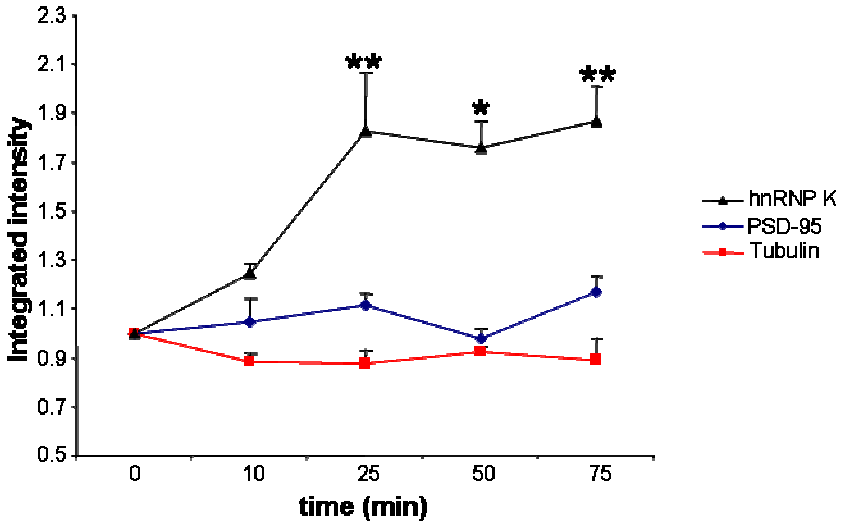

Fig. 14 hnRNP K increase after cLTP. **(A)** Immunoblotting for different markers from neurons treated with glycine; the protein were extracted at different time points after the stimulations. **(B)** Quantification of hnRNP K, PSD-95 and tubulin normalized with the band of GAPDH. The quantification was performed by using of IIMAGEJ software.

Moreover we quantified also the increase of hnRNP K 3 and 6 hours after the glycine treatment (Fig. 15A) to understand if this change in the expression level is persistent over time. To this purpose we induced cLTP in mature hippocampal neurons and we lyseted them 3 or 6 hours afer the treatment. The western blot quantifications showed that the

level of hnRNP K started to decrease 6 hours after glycine, during the L-LTP (NT= 1±0.003; 3h= 1.53±0.06, ***p<0.001; 6h= 1.07±0.03).

Take together these results demonstrate that hnRNP K is required for long-term potentiantion and its silencing blocks this phenomena; moreover, given the role of this protein in regulation of gene expression and mRNA stability and transport, the increase of hnRNP K during the cLTP suggests that it regulates the expression of proteins required for LTP induction.

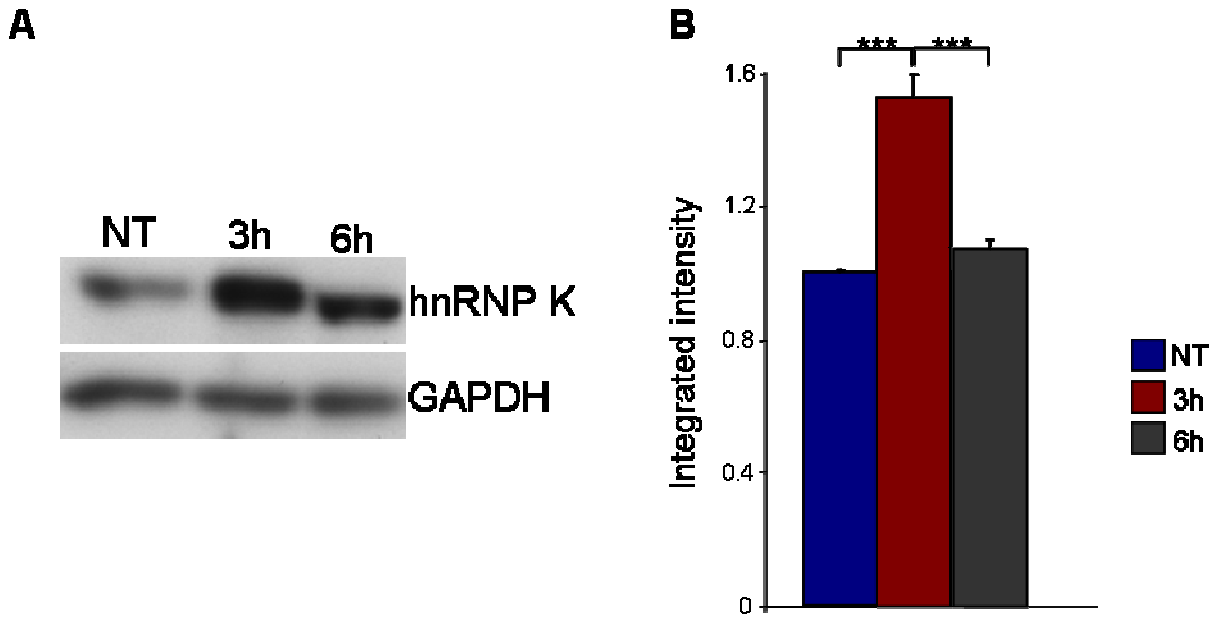

Fig. 15 hnRNP K increase after cLTP. **(A)** Immunoblotting for hnRNP K and GAPDH (to normalize) at different time points after glycine treatment. The increase in hnRNP K level is no longer detectable 6h after cLTP induction **(B)** Quantification performed by using of IIMAGEJ software.

4.4.4 cLTP results in accumulation of hnRNP K in cytoplasm

Subsequently we investigated if the cLTP could induce a change in hnRNP K localization. Hippocampal neurons at DIV18 were treated with glycine for 3 minutes and 40 minutes after the cells were fixed. As it well known, in basal condition, hnRNP K is manly localized in the nucleus, but is also detectable in cytoplasm.

We analyzed the distribution of hnRNP K using an antibody against endogenous protein. We used DAPI to identify the nucleus. As expected, in not treated neurons hnRNP K appeared concentrated in the nucleus, after cLTP treatment the protein is detectable also in cytoplasm.

A

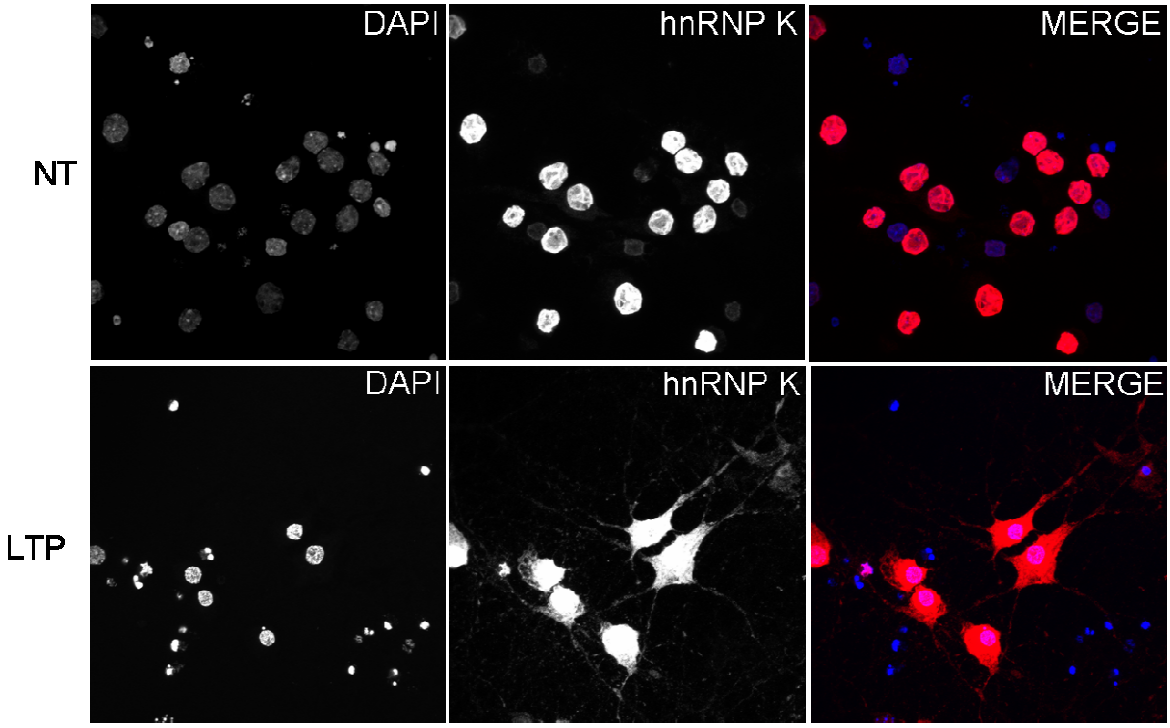

Fig. 16 (A) Change of hnRNP K localization during cLTP. In basal condition hnRNP K appeared concentrated in the nucleus (top panel); 40 min after cLTP induction we observed an enrichment in cytoplasm (bottom panel).

4.5 KEY ROLE OF HNRNP K IN REGULATION OF Arp2/3 COMPLEX

In order to understand how the loss of hnRNP K induces these morphological and functional alterations we focused our attention on the already known interactions of this protein with mRNAs and proteins.

In particular, given the effect on synapses shape and function and on dendrites we investigated in detail the relationship between hnRNP K and actin cytosketon. We found interesting its role in posttranscriptional regulation of Arp2 protein and the interaction with N-WASP, a positive regulator of Arp2/3 complex . In summary, these studyies and our findings seem to indicate an involvement of hnRNP K in actin dynamic.

4.5.1 Direct interaction between hnRNP K and N-WASP in brain

The interaction of overexpressed hnRNP K and N-WASP was already demonstrated in heterologous cells by Yoo Y (Yoo et al., 2006), we riconfermed this interaction in rat brain by co-immunoprecipitation. Co-immunoprecipitation experiments on brain extracts using a polyclonal hnRNP K antibody showed that hnRNP K and N-WASP were associated .
Because N-WASP is implicated in spine formation and morphology (Wegner A 2008), the ability of hnRNP K to associate with N-WASP is in agreement with our finding about the effect of hnRNP K on spine.

A

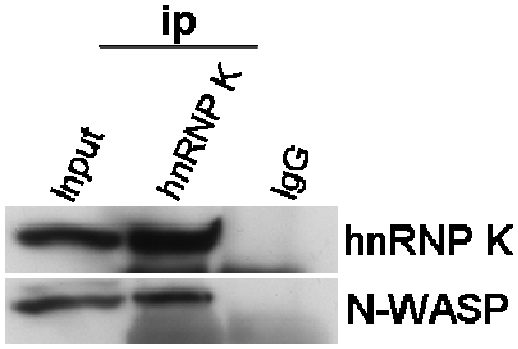

Fig. 17 (A) N-WASP and hnRNP K interaction in neurons. Coimmunoprecipitation experiments on brain extracts using policlonal antibody (bottom panel) show that N-WASP and hnRNP K are associated.

5 DISCUSSION

hnRNP K has been recently involved in the regulation of neuron morphology through its interaction with Abelson-interacting protein 1 (Proepper et al.) and its involvement in actin dynamics. It is known that hnRNP K knockdown is associated with axonal outgrowth block and alterations in neuron morphology (Liu and Szaro, , Liu et al., 2008). The role of hnRNP K in neuron development was supported by the decrease of its expression in brain immediately after birth suggesting that this protein could have a role in the early stages of development; moreover given the persistence of this protein in specific regions of brain linked with learning and memory function (like hippocampus) the purpose of this study was to better characterize the role of this protein in neuron development and function.

The first insight into hnRNP K function derived from the alterations in dendritic tree observed in silenced neurons: in particular the knockdown of hnRNP K led to an impairment in neural arborization (branches complexity and structure) compared to control. This result was in agreement with the downregulation of actin-related protein 2 (Arp2) in the absence of hnRNP K. Arp2 is a component of Arp2/3 complex which has a key role in actin polymerization; its alteration could cause impairments in cytoskeletal structures, like dentrites. Regulation of actin polymerization is crucial for neuronal morphogenesis and function and many structures in neurons are enriched in actin filaments. It is the case of dendritic spines, that form the postsynaptic part of most excitatory synapses and are major sites of information processing and storage in the brain. For this reason we focused our attention on these structures. We found that the density of spines is dramatically decreased in silenced neurons compared to neurons transfected with scrambled, while the spine morphology was not affected. These results suggest that hnRNP K is involved in spine formation and are in good agreement with the evidences of an interaction with N-WASP.N-WASP is another player in actin polymerization and directly interacts with Arp2/3 complex and its involvement in spine formation was already demonstrated. Indeed, N-WASP knockdown in hippocampal neurons induces the same reduction in spine density that we found in hnRNP K adsence (Wegner et al., 2008).
The following analysis on spine showed that these structures in knockdown neurons had a faster turn over compared to control neurons, suggesting that the loss of hnRNP k also induced an alteration in actin structure of spines, making them less stable.

Since N-WASP silencing induces as well a decrease in the number of excitatory synapse we subsequently analyzed the effect of hnRNP K loss on pre- and post-synaptic compartments. To this purpose we performed two different set of experiments. First of all, we quantified the level of different pre- and post-synaptic markers in neurons at DIV 20, that have been transfected at DIV12 with siRNA-hnRNP K or scrambled. We observed a decrease in two postsynaptic markers: PSD-95 and GluA2, a subunit of AMPA receptor. By contrast, no changes were observed in presynaptic markers VGAT and VGLUT; surprisingly NR1, a subunit of the NMDA receptor, and GluA1, a subunit of the AMPA receptor, did not change.

These experiments suggest that hnRNP K is implicated in postsynaptic compartment formation, while the presynaptic is not affected. In particular hnRNP K could have a role in the composition of the PSD, indeed its silencing alters AMPA subunits composition, leaving unchanged other components of the PSD, as NMDA receptors and PICK1.

To further investigate this impairment in the postsynapse we decided to infect neurons with siRNA-hnRNP K or scrambled. We used this approach to be sure that most of the pre- and post-synapses were silenced. We used antibodies against PSD-95 and VGLUT to visualize the synapse. Again, we found a strong alteration in the postsynapse (average area of PSD-95 clusters was decreased) and consequently a reduction in co-localization area between pre- and post-synapse. These results are consistent with the previous evidences about the decrease in postsynaptic markers.

Since the involvement of GluA2 subunit, we performed electrophysiological recordings in order to investigate functional changes in AMPARs physiology. Our results show a dramatic decrease in excitatory, AMPA receptors mediated, miniature postsynaptic currents (mEPSCs) frequency in hnRNP K-silenced neurons. By contrast, currents peak amplitude seemed to be unaffected.

The lower mEPSCs frequency observed in silenced neurons is likely to match (is probably due to) the decrase in spine number described by morphological analysis. Usually, a change in miniature currents frequency is considered an index of some presynaptic effect on neurotransmission (e.g. release probability, number of releasing sites). Nevertheless, in our experiments we had no evidences of changes in presynaptic markers, both from immunocheminstry experiments (VGLUT, VGAT expression) and electrophysiological tools (the change in frequency is not accompanied by a change in the coefficient of variation, as

expected in case of presynaptic involvement). It is likely, then, that this effect is due merely to the loss of spines that characterized silenced dendrites.
Besides, mEPSCs peak amplitude did not show any appreciable change, in silenced neurons compared to scrambled. This is in good agreement with the observation that both size and shape of dendritic spines did not differ in the two conditions. Since spine shape is someway proportional to the number of AMPARs exposed (Lu et al., 2009), and considering that the amplitude of postsynaptic currents is dependent on the abundance of postsynaptic receptors, it is not surprising that the amount of current flowing through the membrane at the peak of miniature events is approximately the same.
Another detail that worth to be discussed here, is the difference in AMPAR subunit composition proposed for silenced and control neurons. The analysis of the decay kinetic of excitatory miniature currents, as well as the quantification of GluA1 and GluA2 in western blot analysis , suggested a change in the physiological balance between GluA1 and GluA2 subunits in AMPARs present in silenced neurons. It is possible that "silenced receptors" are enriched in GluA1 subunits, determining a slower current decay, but leaving the peak amplitude unaffected (in good agreement with Jonas et al. 2000).
Relative to this, it should also be discussed the importance of a change in currents decay kinetics. This parameter is indeed of great relevance for all the processes that concern signals summation and synaptic integration. What could seem a small effect (a few ms delayed signal end) has a profound impact on the whole network efficiency.
This suggests that signals integration and information processing in a network made of neurons lacking hnRNP K should be deeply affected.

In order to understand this aspect we decide to investigate if hnRNP K could have a role in synaptic plasticity. To this purpose we induced cLTP in mature neurons transfected with scrambled or siRNA-hnRNP K and miniature currents were recorded. Interestingly in silenced neurons mEPSCs amplitude did not increase after the induction, showing instead a statistically significant decrease. Surprisingly a similar result was obtained with immunostaining after cLTP induction. The increase of postsynapse area after cLTP has been described (Lu 2001) and for this reason we quantified the area of PSD-95 cluster and colocalization between PSD-95 and VGLUT, taken as an indicator of synaptic potentiation. Also in this case the silenced neurons did not show any increase in PSD-95 cluster; by contrast we observed a decrease similar at synaptic depression.

The glycine-induced cLTP has been described to involve selectively the activation of NMDARs, as a necessary condition for the development of the AMPARs currents potentiation (Lu et al., 2001). Therefore we started to analyze the NMDA component of glutamatergic response, but no difference was found between GFP and silenced signals.
To clarify why in silenced neurons, after glycine treatment, we observed a synaptic depression we will check the increase in intracellular calcium during cLTP induction, through single-cell calcium imaging recordings. Indeed a form of switch between LTP/LTD has been described in hippocampus as dependent to a sort of calcium threshold. For the moment our hypothesis is the following: it is probable that the reduction in miniature currents frequency in silenced neurons, probably due to the poor number of spines detected in morphological analysis, did not allow an increase of intracellular calcium concentration beyond the LTD/LTP threshold.
Anyway it is now evident that hnRNP K is involved in synaptic plasticity, indeed its knockdown prevent the increase of mEPSCs peak amplitude; it remains to understand which is the mechanism that makes hnRNP K necessary for LTP induction.

Modulation of local protein synthesis in neurons plays a key role in the production of long-term, activity dependent changes in synapse structure and functional efficacy. Persistent forms of synaptic change as seen in LTP and LTD typically require rapid gene expression and new protein synthesis. Given the role of hnRNP K in the regulation of protein synthesis, through its involvement in RNA metabolism, we hypothesized that this protein is necessary for new protein synthesis required for the late phase of synaptic plasticity (L-LTP). To validate this idea we looked at the changes in the protein expression at different time points after cLTP induction. Interestingly we observed a strong increase in hnRNP K expression 25 min after the treatment.
It is already known that the early stage of LTP (E-LTP) is protein synthesis-independent, while an enrichment of different proteins was described during the I-LTP and L-LTP. Since we observed an increase of hnRNP K jet immediately after cLTP induction, our hypotheses is that this protein is required for the early phase of long-term potentiation.; this idea is supported by the decrease of hnRNP K immediately after this phase. Its increase was detectable for no longer than 6 hours suggesting that this enrichment is temporary an necessary only for the start of LTP and not for its maintaining.
The importance of hnRNP K in synaptic potentiation was also demonstrated by the change of its localization after glycine treatment. Indeed hnRNP K shifts from the nucleus to the

cytoplasm; probably the recruitment of hnRNP K is necessary to carry out from the nucleus some mRNA required in the L-LTP.

The alterations observed in hnRNP K silenced neurons were described from a morphological and a functional perspective, evidencing a strong impairment of excitatory synaptic structures. Besides, our data suggest a strong link between this protein and actin dynamics, suggesting that these effects could eventually be consequent to the actin cytoskeleton rearrangements caused by hnRNP K loss.

6 BIBLIOGRAPHY

Alarcon, J. M., Hodgman, R., Theis, M., Huang, Y. S., Kandel, E. R. and Richter, J. D., 2004. Selective modulation of some forms of schaffer collateral-CA1 synaptic plasticity in mice with a disruption of the CPEB-1 gene. Learn Mem. 11, 318-327.

Alvarez, V. A. and Sabatini, B. L., 2007. Anatomical and physiological plasticity of dendritic spines. Annu Rev Neurosci. 30, 79-97.

Anantharaman, V., Koonin, E. V. and Aravind, L., 2002. Comparative genomics and evolution of proteins involved in RNA metabolism. Nucleic Acids Res. 30, 1427-1464.

Antar, L. N., Afroz, R., Dictenberg, J. B., Carroll, R. C. and Bassell, G. J., 2004. Metabotropic glutamate receptor activation regulates fragile x mental retardation protein and FMR1 mRNA localization differentially in dendrites and at synapses. J Neurosci. 24, 2648-2655.

Blanchette, A. R., Fuentes Medel, Y. F. and Gardner, P. D., 2006. Cell-type-specific and developmental regulation of heterogeneous nuclear ribonucleoprotein K mRNA in the rat nervous system. Gene Expr Patterns. 6, 596-606.

Bliss, T. V. and Gardner-Medwin, A. R., 1973. Long-lasting potentiation of synaptic transmission in the dentate area of the unanaestetized rabbit following stimulation of the perforant path. J Physiol. 232, 357-374.

Bomsztyk, K., Denisenko, O. and Ostrowski, J., 2004. hnRNP K: one protein multiple processes. Bioessays. 26, 629-638.

Bomsztyk, K., Van Seuningen, I., Suzuki, H., Denisenko, O. and Ostrowski, J., 1997. Diverse molecular interactions of the hnRNP K protein. FEBS Lett. 403, 113-115.

Braddock, D. T., Baber, J. L., Levens, D. and Clore, G. M., 2002. Molecular basis of sequence-specific single-stranded DNA recognition by KH domains: solution structure of a complex between hnRNP K KH3 and single-stranded DNA. Embo J. 21, 3476-3485.

Brandon, J. G. and Coss, R. G., 1982. Rapid dendritic spine stem shortening during one-trial learning: the honeybee's first orientation flight. Brain Res. 252, 51-61.

Brewer, G. J., Torricelli, J. R., Evege, E. K. and Price, P. J., 1993. Optimized survival of hippocampal neurons in B27-supplemented Neurobasal, a new serum-free medium combination. J Neurosci Res. 35, 567-576.

Calabrese, B., Wilson, M. S. and Halpain, S., 2006. Development and regulation of dendritic spine synapses. Physiology (Bethesda). 21, 38-47.

Chelly, J. and Mandel, J. L., 2001. Monogenic causes of X-linked mental retardation. Nat Rev Genet. 2, 669-680.

Citri, A. and Malenka, R. C., 2008. Synaptic plasticity: multiple forms, functions, and mechanisms. Neuropsychopharmacology. 33, 18-41.

Connor, J. R., Beban, S. E., Hopper, P. A., Hansen, B. and Diamond, M. C., 1982. A Golgi study of the superficial pyramidal cells in the somatosensory cortex of socially reared old adult rats. Exp Neurol. 76, 35-45.

de Hoog, C. L., Foster, L. J. and Mann, M., 2004. RNA and RNA binding proteins participate in early stages of cell spreading through spreading initiation centers. Cell. 117, 649-662.

Dejgaard, K., Leffers, H., Rasmussen, H. H., Madsen, P., Kruse, T. A., Gesser, B., Nielsen, H. and Celis, J. E., 1994. Identification, molecular cloning, expression and chromosome mapping of a family of transformation upregulated hnRNP-K proteins derived by alternative splicing. J Mol Biol. 236, 33-48.

Du, L. and Richter, J. D., 2005. Activity-dependent polyadenylation in neurons. Rna. 11, 1340-1347.

Elste, A. M. and Benson, D. L., 2006. Structural basis for developmentally regulated changes in cadherin function at synapses. J Comp Neurol. 495, 324-335.

Expert-Bezancon, A., Le Caer, J. P. and Marie, J., 2002. Heterogeneous nuclear ribonucleoprotein (hnRNP) K is a component of an intronic splicing enhancer complex that activates the splicing of the alternative exon 6A from chicken beta-tropomyosin pre-mRNA. J Biol Chem. 277, 16614-16623.

Fiala, J. C., Spacek, J. and Harris, K. M., 2002. Dendritic spine pathology: cause or consequence of neurological disorders? Brain Res Brain Res Rev. 39, 29-54.

Gabut, M., Chaudhry, S. and Blencowe, B. J., 2008. SnapShot: The splicing regulatory machinery. Cell. 133, 192 e191.

Glisovic, T., Bachorik, J. L., Yong, J. and Dreyfuss, G., 2008. RNA-binding proteins and post-transcriptional gene regulation. FEBS Lett. 582, 1977-1986.

Globus, A. and Scheibel, A. B., 1967. The effect of visual deprivation on cortical neurons: a Golgi study. Exp Neurol. 19, 331-345.

Goley, E. D. and Welch, M. D., 2006. The ARP2/3 complex: an actin nucleator comes of age. Nat Rev Mol Cell Biol. 7, 713-726.

Greenough, W. T. and Volkmar, F. R., 1973. Pattern of dendritic branching in occipital cortex of rats reared in complex environments. Exp Neurol. 40, 491-504.

Grutzendler, J., Kasthuri, N. and Gan, W. B., 2002. Long-term dendritic spine stability in the adult cortex. Nature. 420, 812-816.

Higashi, S., Iseki, E., Yamamoto, R., Minegishi, M., Hino, H., Fujisawa, K., Togo, T., Katsuse, O., Uchikado, H., Furukawa, Y., Kosaka, K. and Arai, H., 2007. Concurrence of TDP-43, tau and alpha-synuclein pathology in brains of Alzheimer's disease and dementia with Lewy bodies. Brain Res. 1184, 284-294.

Honkura, N., Matsuzaki, M., Noguchi, J., Ellis-Davies, G. C. and Kasai, H., 2008. The subspine organization of actin fibers regulates the structure and plasticity of dendritic spines. Neuron. 57, 719-729.

Hotulainen, P. and Hoogenraad, C. C., Actin in dendritic spines: connecting dynamics to function. J Cell Biol. 189, 619-629.

Hotulainen, P., Llano, O., Smirnov, S., Tanhuanpaa, K., Faix, J., Rivera, C. and Lappalainen, P., 2009. Defining mechanisms of actin polymerization and depolymerization during dendritic spine morphogenesis. J Cell Biol. 185, 323-339.

Huang, C. S., Shi, S. H., Ule, J., Ruggiu, M., Barker, L. A., Darnell, R. B., Jan, Y. N. and Jan, L. Y., 2005. Common molecular pathways mediate long-term potentiation of synaptic excitation and slow synaptic inhibition. Cell. 123, 105-118.

Huang, Y. S., Jung, M. Y., Sarkissian, M. and Richter, J. D., 2002. N-methyl-D-aspartate receptor signaling results in Aurora kinase-catalyzed CPEB phosphorylation and alpha CaMKII mRNA polyadenylation at synapses. Embo J. 21, 2139-2148.

Huber, K. M., Gallagher, S. M., Warren, S. T. and Bear, M. F., 2002. Altered synaptic plasticity in a mouse model of fragile X mental retardation. Proc Natl Acad Sci U S A. 99, 7746-7750.

Jedlicka, P., Vlachos, A., Schwarzacher, S. W. and Deller, T., 2008. A role for the spine apparatus in LTP and spatial learning. Behav Brain Res. 192, 12-19.

Jonas, P., 2000. The Time Course of Signaling at Central Glutamatergic Synapses. News Physiol Sci. 15, 83-89.

Kamma, H., Portman, D. S. and Dreyfuss, G., 1995. Cell type-specific expression of hnRNP proteins. Exp Cell Res. 221, 187-196.

Kasai, H., Matsuzaki, M., Noguchi, J., Yasumatsu, N. and Nakahara, H., 2003. Structure-stability-function relationships of dendritic spines. Trends Neurosci. 26, 360-368.

Kim, E. and Ko, J., 2006. Molecular organization and assembly of the postsynaptic density of excitatory brain synapses. Results Probl Cell Differ. 43, 1-23.

Kim, E. and Sheng, M., 2009. The postsynaptic density. Curr Biol. 19, R723-724.

Kim, M. J., Futai, K., Jo, J., Hayashi, Y., Cho, K. and Sheng, M., 2007. Synaptic accumulation of PSD-95 and synaptic function regulated by phosphorylation of serine-295 of PSD-95. Neuron. 56, 488-502.

Kirov, S. A., Sorra, K. E. and Harris, K. M., 1999. Slices have more synapses than perfusion-fixed hippocampus from both young and mature rats. J Neurosci. 19, 2876-2886.

Koekkoek, S. K., Yamaguchi, K., Milojkovic, B. A., Dortland, B. R., Ruigrok, T. J., Maex, R., De Graaf, W., Smit, A. E., VanderWerf, F., Bakker, C. E., Willemsen, R., Ikeda, T., Kakizawa, S., Onodera, K., Nelson, D. L., Mientjes, E., Joosten, M., De Schutter, E., Oostra, B. A., Ito, M. and De Zeeuw, C. I., 2005. Deletion of FMR1 in Purkinje cells enhances parallel fiber LTD, enlarges spines, and attenuates cerebellar eyelid conditioning in Fragile X syndrome. Neuron. 47, 339-352.

Korobova, F. and Svitkina, T., Molecular architecture of synaptic actin cytoskeleton in hippocampal neurons reveals a mechanism of dendritic spine morphogenesis. Mol Biol Cell. 21, 165-176.

Lamprecht, R. and LeDoux, J., 2004. Structural plasticity and memory. Nat Rev Neurosci. 5, 45-54.

Landis, D. M. and Reese, T. S., 1983. Cytoplasmic organization in cerebellar dendritic spines. J Cell Biol. 97, 1169-1178.

Liu, Y., Gervasi, C. and Szaro, B. G., 2008. A crucial role for hnRNP K in axon development in Xenopus laevis. Development. 135, 3125-3135.

Liu, Y. and Szaro, B. G., hnRNP K post-transcriptionally co-regulates multiple cytoskeletal genes needed for axonogenesis. Development. 138, 3079-3090.

Lu, W., Man, H., Ju, W., Trimble, W. S., MacDonald, J. F. and Wang, Y. T., 2001. Activation of synaptic NMDA receptors induces membrane insertion of new AMPA receptors and LTP in cultured hippocampal neurons. Neuron. 29, 243-254.

Lu, W., Shi, Y., Jackson, A. C., Bjorgan, K., During, M. J., Sprengel, R., Seeburg, P. H. and Nicoll, R. A., 2009. Subunit composition of synaptic AMPA receptors revealed by a single-cell genetic approach. Neuron. 62, 254-268.

Lukong, K. E., Chang, K. W., Khandjian, E. W. and Richard, S., 2008. RNA-binding proteins in human genetic disease. Trends Genet. 24, 416-425.

Lunde, B. M., Moore, C. and Varani, G., 2007. RNA-binding proteins: modular design for efficient function. Nat Rev Mol Cell Biol. 8, 479-490.

Majewska, A., Tashiro, A. and Yuste, R., 2000. Regulation of spine calcium dynamics by rapid spine motility. J Neurosci. 20, 8262-8268.

Matsuoka, S., Ballif, B. A., Smogorzewska, A., McDonald, E. R., 3rd, Hurov, K. E., Luo, J., Bakalarski, C. E., Zhao, Z., Solimini, N., Lerenthal, Y., Shiloh, Y., Gygi, S. P. and Elledge, S. J., 2007. ATM and ATR substrate analysis reveals extensive protein networks responsive to DNA damage. Science. 316, 1160-1166.

Matsuzaki, M., Honkura, N., Ellis-Davies, G. C. and Kasai, H., 2004. Structural basis of long-term potentiation in single dendritic spines. Nature. 429, 761-766.

McKee, A. E., Minet, E., Stern, C., Riahi, S., Stiles, C. D. and Silver, P. A., 2005. A genome-wide in situ hybridization map of RNA-binding proteins reveals anatomically restricted expression in the developing mouse brain. BMC Dev Biol. 5, 14.

McKinney, R. A., Capogna, M., Durr, R., Gahwiler, B. H. and Thompson, S. M., 1999. Miniature synaptic events maintain dendritic spines via AMPA receptor activation. Nat Neurosci. 2, 44-49.

Michelotti, E. F., Michelotti, G. A., Aronsohn, A. I. and Levens, D., 1996. Heterogeneous nuclear ribonucleoprotein K is a transcription factor. Mol Cell Biol. 16, 2350-2360.

Miki, H., Miura, K. and Takenawa, T., 1996. N-WASP, a novel actin-depolymerizing protein, regulates the cortical cytoskeletal rearrangement in a PIP2-dependent manner downstream of tyrosine kinases. Embo J. 15, 5326-5335.

Neumann, M., Sampathu, D. M., Kwong, L. K., Truax, A. C., Micsenyi, M. C., Chou, T. T., Bruce, J., Schuck, T., Grossman, M., Clark, C. M., McCluskey, L. F., Miller, B. L., Masliah, E., Mackenzie, I. R., Feldman, H., Feiden, W., Kretzschmar, H. A., Trojanowski, J. Q. and Lee, V. M., 2006. Ubiquitinated TDP-43 in frontotemporal lobar degeneration and amyotrophic lateral sclerosis. Science. 314, 130-133.

Nusser, Z., Hajos, N., Somogyi, P. and Mody, I., 1998. Increased number of synaptic GABA(A) receptors underlies potentiation at hippocampal inhibitory synapses. Nature. 395, 172-177.

Ostrowski, J., Kawata, Y., Schullery, D. S., Denisenko, O. N. and Bomsztyk, K., 2003. Transient recruitment of the hnRNP K protein to inducibly transcribed gene loci. Nucleic Acids Res. 31, 3954-3962.

Papa, M., Bundman, M. C., Greenberger, V. and Segal, M., 1995. Morphological analysis of dendritic spine development in primary cultures of hippocampal neurons. J Neurosci. 15, 1-11.

Parnavelas, J. G., Globus, A. and Kaups, P., 1973. Continuous illumination from birth affects spine density of neurons in the visual cortex of the rat. Exp Neurol. 40, 742-747.

Passafaro, M., Nakagawa, T., Sala, C. and Sheng, M., 2003. Induction of dendritic spines by an extracellular domain of AMPA receptor subunit GluR2. Nature. 424, 677-681.

Peters, A. and Kaiserman-Abramof, I. R., 1970. The small pyramidal neuron of the rat cerebral cortex. The perikaryon, dendrites and spines. Am J Anat. 127, 321-355.

Pollard, T. D. and Borisy, G. G., 2003. Cellular motility driven by assembly and disassembly of actin filaments. Cell. 112, 453-465.

Proepper, C., Steinestel, K., Schmeisser, M. J., Heinrich, J., Steinestel, J., Bockmann, J., Liebau, S. and Boeckers, T. M., Heterogeneous nuclear ribonucleoprotein k interacts with Abi-1 at postsynaptic sites and modulates dendritic spine morphology. PLoS One. 6, e27045.

Purpura, D. P., 1974. Dendritic spine "dysgenesis" and mental retardation. Science. 186, 1126-1128.

Racz, B., Blanpied, T. A., Ehlers, M. D. and Weinberg, R. J., 2004. Lateral organization of endocytic machinery in dendritic spines. Nat Neurosci. 7, 917-918.

Racz, B. and Weinberg, R. J., 2008. Organization of the Arp2/3 complex in hippocampal spines. J Neurosci. 28, 5654-5659.

Rohatgi, R., Ma, L., Miki, H., Lopez, M., Kirchhausen, T., Takenawa, T. and Kirschner, M. W., 1999. The interaction between N-WASP and the Arp2/3 complex links Cdc42-dependent signals to actin assembly. Cell. 97, 221-231.

Rumbaugh, G. and Vicini, S., 1999. Distinct synaptic and extrasynaptic NMDA receptors in developing cerebellar granule neurons. J Neurosci. 19, 10603-10610.

Scheiffele, P., 2003. Cell-cell signaling during synapse formation in the CNS. Annu Rev Neurosci. 26, 485-508.

Schikorski, T. and Stevens, C. F., 1999. Quantitative fine-structural analysis of olfactory cortical synapses. Proc Natl Acad Sci U S A. 96, 4107-4112.

Sheng, M. and Hoogenraad, C. C., 2007. The postsynaptic architecture of excitatory synapses: a more quantitative view. Annu Rev Biochem. 76, 823-847.

Sheng, M. and Kim, M. J., 2002. Postsynaptic signaling and plasticity mechanisms. Science. 298, 776-780.

Sholl, D. A., 1953. Dendritic organization in the neurons of the visual and motor cortices of the cat. J Anat. 87, 387-406.

Si, K., Giustetto, M., Etkin, A., Hsu, R., Janisiewicz, A. M., Miniaci, M. C., Kim, J. H., Zhu, H. and Kandel, E. R., 2003. A neuronal isoform of CPEB regulates local protein synthesis and stabilizes synapse-specific long-term facilitation in aplysia. Cell. 115, 893-904.

Siomi, H., Matunis, M. J., Michael, W. M. and Dreyfuss, G., 1993. The pre-mRNA binding K protein contains a novel evolutionarily conserved motif. Nucleic Acids Res. 21, 1193-1198.

Sudhof, T. C., 2004. The synaptic vesicle cycle. Annu Rev Neurosci. 27, 509-547.

Valverde, F., 1967. Apical dendritic spines of the visual cortex and light deprivation in the mouse. Exp Brain Res. 3, 337-352.

Valverde, F., 1971. Rate and extent of recovery from dark rearing in the visual cortex of the mouse. Brain Res. 33, 1-11.

Wang, G. S. and Cooper, T. A., 2007. Splicing in disease: disruption of the splicing code and the decoding machinery. Nat Rev Genet. 8, 749-761.

Wegner, A. M., Nebhan, C. A., Hu, L., Majumdar, D., Meier, K. M., Weaver, A. M. and Webb, D. J., 2008. N-wasp and the arp2/3 complex are critical regulators of actin in the development of dendritic spines and synapses. J Biol Chem. 283, 15912-15920.

Weiler, I. J., Spangler, C. C., Klintsova, A. Y., Grossman, A. W., Kim, S. H., Bertaina-Anglade, V., Khaliq, H., de Vries, F. E., Lambers, F. A., Hatia, F., Base, C. K. and Greenough, W. T., 2004. Fragile X mental retardation protein is necessary for neurotransmitter-activated protein translation at synapses. Proc Natl Acad Sci U S A. 101, 17504-17509.

Yano, M., Okano, H. J. and Okano, H., 2005. Involvement of Hu and heterogeneous nuclear ribonucleoprotein K in neuronal differentiation through p21 mRNA post-transcriptional regulation. J Biol Chem. 280, 12690-12699.

Yoo, Y., Wu, X., Egile, C., Li, R. and Guan, J. L., 2006. Interaction of N-WASP with hnRNPK and its role in filopodia formation and cell spreading. J Biol Chem. 281, 15352-15360.

Yuste, R. and Bonhoeffer, T., 2001. Morphological changes in dendritic spines associated with long-term synaptic plasticity. Annu Rev Neurosci. 24, 1071-1089.

Yuste, R., Majewska, A. and Holthoff, K., 2000. From form to function: calcium compartmentalization in dendritic spines. Nat Neurosci. 3, 653-659.

Zhang, G., Neubert, T. A. and Jordan, B. A., RNA binding proteins accumulate at the postsynaptic density with synaptic activity. J Neurosci. 32, 599-609.